ISSN 1075-7015, Geology of Ore Deposits, 2023, Vol. 65, No. 8, pp. 827–846. © Pleiades Publishing, Ltd., 2023.
Russian Text © The Author(s), 2022, published in Zapiski Rossiiskogo Mineralogicheskogo Obshchestva, 2022, No. 3, pp. 96–122.

Langbeinite-Group Minerals and Vanthoffite from Fumarole Exhalations of the Tolbachik Volcano (Kamchatka)

M. O. Bulakh[a], *, I. V. Pekov[a], N. N. Koshlyakova[a], S. N. Britvin[b], and M. A. Nazarova[c]

[a] *Moscow State University, Moscow, 119991 Russia*

[b] *St. Petersburg State University, St. Petersburg, 199034 Russia*

[c] *Institute of Volcanology and Seismology, Far East Branch, Russian Academy of Sciences, Petropavlovsk-Kamchatsky, 683006 Russia*

**e-mail: aregon27@mail.ru*

Received May 20, 2022; revised May 23, 2022; accepted May 23, 2022

Abstract—In this paper, we provide characteristics of sulfates of exhalation origin—langbeinite $K_2Mg_2(SO_4)_3$, two modifications of calciolangbeinite $K_2Ca_2(SO_4)_3$ (new data), and vanthoffite $Na_6Mg(SO_4)_4$ (first mineralogical data for this genetic type)—from active fumaroles of the Tolbachik volcano in Kamchatka. These minerals are associated with anhydrous copper sulfates and arsenates, minerals of the aphthitalite and alluaudite groups, krasheninnikovite, anhydrite, sanidine, cristobalite, tridymite, tenorite, hematite, etc. Langbeinite and calciolangbeinite form a series of solid solutions, in which most of the compositions correspond to the ranges of $(Mg_{2.0-1.6}Ca_{0.0-0.4})$ and $(Ca_{1.2-2.0}Mg_{0.8-0.0})$. It is shown that, in calciolangbeinite, with a content of more than 20 mol % of $K_2Mg_2(SO_4)_3$, decomposition into cubic calciolangbeinite with a lower Mg content and langbeinite can occur upon slow cooling. For the first time, in minerals of the langbeinite group, impurities of copper and zinc, the maximal concentrations of which are noted in langbeinite with a low Ca content and reach 0.53 atoms per formula unit (below, apfu) for Zn (10.0 wt % of ZnO) and 0.18 apfu for Cu (3.3 wt % of CuO), were revealed. These elements replace Mg and Ca. Varieties of langbeinite and calciolangbeinite enriched in Na (up to 0.31 apfu = 2.3 wt % of Na_2O) were found. Other significant impurities in these minerals are represented by Rb, Cs, Mn, Cd, Al, and Fe. The fumarole vanthoffite contains impurities of K, Ca, Mn, Zn, Cu, and Fe (up to 0.47 apfu in total). This significant manifestation of cationic isomorphism in langbeinite-group minerals and vanthoffite is observed only at Tolbachik volcano and is caused primarily with the peculiar conditions of their crystallization in high-temperature volcanic fumaroles.

Keywords: langbeinite, calciolangbeinite, vanthoffite, fumarole, Tolbachik volcano, Raman spectrum

DOI: 10.1134/S1075701523080032

The langbeinite group combines five natural double sulfates with the general formula $A_2^+M_2^{2+}(SO_4)_3$: langbeinite $K_2Mg_2(SO_4)_3$, manganolangbeinite $K_2Mn_2(SO_4)_3$, calciolangbeinite $K_2Ca_2(SO_4)_3$, efremovite $(NH_4)_2Mg_2(SO_4)_3$, and ferroefremovite $(NH_4)_2Fe_2^{2+}(SO_4)_3$. All these minerals have a cubic syngony and space group $P2_13$. Only in calciolangbeinite, as we recently showed, two polymorphic modifications were established in nature: cubic calciolangbeinite-*C* (space group $P2_13$) and orthorhombic calciolangbeinite-*O* ($P2_12_12_1$). They have the same structural topology and, for this reason, are considered as structural varieties of the mineral type of calciolangbeinite, despite noticeable differences in radiographic characteristics and properties (Pekov et al., 2022).

The crystal structures of all these minerals are based on a framework of distorted MO_6 octahedra of two types and SO_4 tetrahedra connected by vertices and alternating with each other. Large *A* cations, which also occupy two crystallographically nonequivalent positions with coordination numbers IX and X, are located in the cavities of the framework (Zemann and Zemann, 1957; Gattow and Zemann, 1958; Mereiter, 1979; Yamada et al., 1981; Speer and Salje, 1986; Pekov et al., 2012, 2022).

Among synthetic compounds, a number of sulfates with the langbeinite structure, in which octahedrally coordinated cations are represented by Ca^{2+}, Mg^{2+}, Mn^{2+}, Fe^{2+}, Co^{2+}, Ni^{2+}, Zn^{2+}, and Cd^{2+}, while K^+, Rb^+, Cs^+, Tl^+, or NH_4^+ predominate in the large-cation position, are known. Langbeinite-like phases with tetrahedral anionic complexes $(CrO_4)^{2-}$, $(SeO_4)^{2-}$, $(MoO_4)^{2-}$, $(PO_4)^{3-}$, and $(AsO_4)^{3-}$ were also synthesized. In the last two cases, electrical neutrality is ensured by the presence of tri- or tetravalent cations: Sc^{3+}, Cr^{3+}, REE^{3+}, Ti^{4+}, Zr^{4+}, and Sn^{4+} in the octahedral position (Abrahams and Bernstain, 1977; Hikita

et al., 1980; Yamada et al., 1981; Latush et al., 1983; Devarajan and Salje, 1984; Speer and Salje, 1986; Vlokh et al., 2004; Zapeka et al., 2013; Lander et al., 2017; Martynov et al., 2017).

Langbeinite was first described in 1891 in samples from the Wilhelmshall salt mine (Harz, Germany). The name of the mineral was given in honor of Adalbert Langbein, director of a chemical factory in Stassfurt, Germany (Zuckschwerdt, 1891). Langbeinite is relatively widespread in marine evaporite deposits containing deposits of potassium salts. In some deposits (Stebnikskoe and Kalush-Golynskoe in Ukraine, as well as Carlsbad in New Mexico in the United States), it forms industrial-scale accumulations and serves as an important component of potash ores. In evaporites, langbeinite occurs in association with halite, sylvin, epsomite, polyhalite, kieserite, and, sometimes, with carnallite and aphthitalite, forming continuous masses, grains, filamentous aggregates, and, sometimes, crystals with a tetrahedral habit (Korobtsova, 1955; Stewart, 1963; Khod'kova, 1968; Ivanov and Voronova, 1972; Vishnyakov et al., 2016). Langbeinite of exhalation origin is also known. For example, in the literature, there are data on its findings in the fumaroles of volcanoes of the Central American arc: Izalco in El Salvador, Pacaya and Santiagito in Guatemala, and Momotombo and Cerro Negro in Nicaragua. There, this mineral was described together with aphthitalite and hexagonal Na sulfate (metatenardite) in fumarole chambers with a temperature of 400–900°C, as well as in associations with anhydrite, thenardite, aphthitalite, chalcokyanite, and anglesite in lower temperature (100–200°C) zones of fumaroles (Stoiber and Rose, 1974). At the Icelandic volcanoes Eldfell and Fimmverdyhauls, langbeinite occurs in fumaroles with a temperature of 80–230°C as white crusts covering volcanic scoria (Balić-Žunić et al., 2016). In fumarolic exhalations of the Tolbachik volcano in Kamchatka, this sulfate was first noted in the early 1990s (Vergasova and Filatov, 1993), but was not described until now. Langbeinite is also found in gas sublimates of technogenic analogues of volcanic fumaroles, in the burnt dumps of coal-mining enterprises of the Chelyabinsk coal basin in the Southern Urals (Chesnokov and Shcherbakova, 1991) and in the burning coal mines of Avignon in France (Masalehdani et al., 2009).

The Mn-dominant analog of langbeinite, manganolangbeinite, was found in 1922 in fumarole exhalations of the Vesuvius volcano in Italy in association with thenardite, halite, and aphthalite (Zambonini and Carobbi, 1924; Bellanca, 1947). No other finds were reported.

Cubic calciolangbeinite was first discovered in exhalations of the Yadovitaya fumarole on the Tolbachik volcano (Pekov et al., 2012). A little later, a rhombic modification of this sulfate was found in the neighboring Arsenatnaya fumarole. Almost simultaneously, it was found in the pyrometamorphic rocks of the Hatrurim Complex in Israel and Palestine, where it occurs together with aphthitalite, thenardite, larnite, fluorellestadite, gehlenite, and ternesite (Galuskina et al., 2014; Galuskin et al., 2016; Pekov et al., 2022); the cubic modification of calciolangbeinite was not found in Hatrurim.

The first ammonium representative of the group, efremovite, was discovered in the burnt dumps of the Chelyabinsk coal basin in the Southern Urals in 1985. It was found in technogenic pseudofumaroles in association with native sulfur, cladnoite, and mascanite (Shcherbakova and Bazhenova, 1989). It has also been found in other similar objects: in pseudofumaroles of burning coal mines in the Czech Republic (Sejkora and Kotrlý, 2001), Hungary (Szakáll and Kristály, 2008), Silesia in Poland (Parafiniuk and Kruszewski, 2009), Hokkaido in Japan (Shimobayashi et al., 2011). Under natural conditions, efremovite was reliably recorded only in exhalations of the Bocca Grande fumarole in the Phlegraean fields (Italy), where it occurs together with huisingite–(Al) and bussengotite (Russo et al., 2017). There, in association with opal, godovikite, adranosite, huisingite–(Al), and mascaignite, its ferruginous analogue, ferroefremovite, was recently described (Kasatkin et al., 2021).

Most of published chemical analyses of langbeinite-group minerals refer actually to langbeinite and calciolangbeinite from Tolbachik fumarolic exhalations (Pekov et al., 2012, 2022). In the last study, we briefly characterized a series of solid solutions between Tolbachik langbeinite and calciolangbeinite. It was found that the Ca-dominant members of the series containing more than 0.1 atoms per formula (hereinafter, referred to as the a.f.) of Mg refer to the cubic modification while the samples of the $K_2(Ca_{2.0-1.9}Mg_{0.0-0.1})(SO_4)_3$ composition have a orthorhombic structure. The presence of other chemical components (impurities) in these sulfates is actually only mentioned in (Pekov et al., 2012, 2022).

Information about isomorphism in minerals of the langbeinite group from other objects is very scarce. Chemical analyses of langbeinite from evaporite deposits available in the literature are few in number (Zuckschwerdt, 1891; Korobtsova, 1955; Anthony et al., 2003) and characterize this sulfate as a chemically quite pure compound, which is also confirmed by our data (electron-probe analysis of langbeinite from the Stebnik deposit is given in Table 1). Only small impurities of iron (0.40 wt % of Fe_2O_3) and manganese (~0.03 wt % of MnO) in langbeinite from the salt deposits of the Carpathian region are noted by Korobtsova (1955). The features of the chemical composition are not described for langbeinite from volcanic fumaroles and their technogenic analogs, as well as for manganolangbeinite (with the exception of the already mentioned data on the Tolbachik samples). In calciolangbeinite-*O* from the pyrometamorphic rocks

Table 1. (1) Chemical composition of langbeinite from the Stebnik potassium salt deposit (Ukraine) and (12–14) fumarolic exhalations of the Tolbachik volcano (Kamchatka, Russia)

	1	2	3	4	5	6	7	8	9	10	11	12	13	14
	wt %													
Na_2O		0.47	2.27	1.08	0.64	0.46	2.07	2.00	0.28	0.59		0.34	0.90	0.32
K_2O	23.05	22.49	20.09	20.97	21.31	20.34	17.58	17.44	21.80	21.53	21.58	21.66	21.00	20.71
Rb_2O		0.25		0.56	0.25	0.81	1.38	0.96	0.40	0.61	0.25	0.29	0.23	0.16
MgO	19.09	18.50	17.54	17.10	16.90	13.94	13.18	13.02	16.34	16.49	15.12	15.94	15.99	14.87
CaO		0.20	0.13	0.18	0.45	0.48	0.22	0.30	1.90	2.66	3.40	3.44	4.13	5.25
MnO				0.20	0.41	0.42	0.48	0.49	0.51		0.18	0.41	0.19	0.37
CuO				0.40	1.94	3.31	1.22	1.52			1.04	0.79		0.64
ZnO			1.31	2.16	0.61	5.93	8.42	9.99	0.47	0.85	1.23	0.40		0.41
Al_2O_3							0.10		0.09					
Fe_2O_3					0.40				1.80					0.27
SO_3	58.35	57.49	57.59	57.41	57.03	55.16	54.65	55.16	56.43	57.07	57.12	56.72	58.55	57.74
Sum	100.49	99.40	98.92	100.06	99.94	100.85	99.30	100.88	100.02	99.80	99.92	99.99	100.99	100.74
	Formula coefficients per 12 O atoms													
K	2.02	2.00	1.79	1.87	1.91	1.87	1.64	1.61	1.97	1.93	1.94	1.94	1.84	1.84
Na			0.22	0.08	0.05	0.06	0.29	0.28	0.02	0.05		0.04	0.07	0.04
Rb		0.01		0.03	0.01	0.04	0.06	0.04	0.02	0.03	0.01	0.01	0.01	0.01
Ca						0.04	0.02	0.02				0.02		0.01
$\sum A$	2.02	2.01	2.01	1.98	1.97	2.01	2.01	1.95	2.01	2.01	1.95	2.01	1.92	1.90
Na		0.06	0.09	0.07	0.04				0.02	0.03		0.01	0.05	
Mg	1.96	1.92	1.83	1.78	1.77	1.50	1.44	1.40	1.73	1.73	1.59	1.67	1.64	1.54
Ca		0.01	0.01	0.01	0.03				0.14	0.20	0.26	0.24	0.30	0.38
Mn				0.01	0.02	0.03	0.03	0.03	0.03		0.01	0.02	0.01	0.02
Cu				0.02	0.10	0.18	0.07	0.08			0.06	0.04		0.03
Zn			0.07	0.11	0.03	0.32	0.45	0.53	0.02	0.04	0.06	0.02		0.02
Al							0.01		0.01					
Fe					0.01				0.05					0.01
$\sum M$	1.96	1.99	2.00	2.00	2.00	2.03	2.00	2.04	2.00	2.00	1.98	2.00	2.00	2.00
$\sum Me$	3.98	4.00	4.01	3.98	3.97	4.04	4.01	3.99	4.01	4.01	3.93	4.01	3.92	3.90
S^{6+}	3.01	3.01	3.02	3.01	3.01	2.99	3.00	2.99	3.00	3.01	3.02	2.99	3.02	3.01

ΣM = Mg + Ca + ^{M}Na + Mn + Cu + Zn + Al + Fe. ΣA = K + ^{A}Na + Rb + ^{A}Ca; ΣMe is the sum of all metals. An empty cell indicates the content of the component below the detection limit. an. 2, 4, 6–8, 10, 11, 13, Arsenatnaya fumarole; an. 5, 9, 12, 14, Yadovitaya fumarole; an. 3, fumarole Main Tenoritovaya.

of the Hatrurim complex, the content of impurities turned out to be below the detection threshold by the electron probe method (Pekov et al., 2022). Regarding impurities in the ammonium members of the group, it is known that the empirical formula of efremovite from the burnt dumps of the Chelyabinsk coal basin is $((NH_4)_{2.00}K_{0.06}Na_{0.02})_{\Sigma 2.08}(Mg_{1.79}Fe^{2+}_{0.06}Ca_{0.04}Mn_{0.02})_{\Sigma 1.91}S_{3.01}O_{12}$ (Shcherbakova and Bazhenova, 1989) while the composition of ferroefremovite from exhalations of the Phlegraean fields corresponds to the formula $(NH_4)_{1.85}K_{0.12}Na_{0.01})_{\Sigma 1.98}(Fe^{2+}_{1.11}Mg_{0.87}Mn_{0.06})_{\Sigma 2.04}S_{2.99}O_{12}$ (Kasatkin et al., 2021).

Another magnesian–alkaline sulfate, vanthoffite $Na_6Mg(SO_4)_4$, is known in the fumarole exhalations of Tolbachik. As langbeinite, this mineral was discovered in the Wilhelmshall salt mine in Harz (Germany) in 1902 and was named after the famous Dutch chemist J.Kh. van't Hoff (Kubierschky, 1902).

Vanthoffite has a monoclinic syngony and space group $P2_1/c$. The crystal structure of $Na_6Mg(SO_4)_4$ was first determined in 1964 using a synthetic sample (Fischer and Hellner, 1964), and later refined using natural vanthoffite (Balić-Žunić et al., 2020). Mg atoms center weakly distorted oxygen octahedra, while

Na atoms are in three nonequivalent positions: in distorted octahedra and in two types of seven vertices, which are close in configuration to a pentagonal dipyramid. Sulfate tetrahedra and cationic polyhedra form two types of layers. In layers of the first type, (MgO_6) octahedra alternate with sulfate tetrahedra, forming chains, the space between which inside the layer is occupied by ($Na(1)O_7$) polyhedra connected in pairs by common edges. Layers of the second type form chains of ($Na(2)O_7$) polyhedra, which are connected by common edges with ($Na(3)O_6$) octahedra and with another part of sulfate tetrahedra (Fischer and Hellner, 1964; Balić-Žunić et al., 2020).

Vanthoffite occurs in marine evaporite deposits, where it mainly associates with halite, sylvite, carnallite, langbeinite, bledite, and leveite (Ivanov and Voronova, 1972; Anthony et al., 2003; Babel and Schreiber, 2014). This sulfate was also noted in fumarole exhalations: on the Eldfell and Fimmverduhauls volcanoes in Iceland, where it is found in association with glauberite, thenardite, and leveite (Mitolo et al., 2008; Balić-Žunić et al., 2016) and on Tolbachik (Pekov et al., 2015; Shchipalkina et al., 2021), but no descriptions of exhalation vanthoffite were provided.

Vanthoffite from evaporite deposits does not contain isomorphic impurities in any significant amounts (Kubierschky, 1902; Nguyen et al., 1973; Anthony et al., 2003). The only published analysis of exhalation vanthoffite from the Arsenatnaya fumarole on Tolbachik (Shchipalkina et al., 2021) found CuO in an amount of 4.4 wt % and ZnO in an amount of 2.0 wt %, as well as MnO and CaO in an amount of 0.2 wt %.

We studied in detail over a hundred samples of minerals of the langbeinite and vanthoffite groups from the active fumaroles of the Tolbachik volcano. Only a small amount of obtained data, mainly related to the chemical composition and crystal chemistry of calciolangbeinite, were previously published (Pekov et al., 2012, 2022). In this study, the conditions for the occurrence and morphological diversity of these sulfates and the specifics of their chemical composition with an emphasis on the distribution of impurity cations are systematically characterized. The results of X-ray and Raman spectroscopic studies are also presented. In this paper, the mineralogical characteristics of exhalation vanthoffite are given for the first time.

OCCURRENCE AND MORPHOLOGY

Tolbachik, which is part of the Klyuchevskaya volcano group in the northern part of the Eastern Volcanic Belt of Kamchatka, is a volcanic massif that includes the extinct volcano Ostryi Tolbachik, active basalt volcano Plosky Tolbachik, and Tolbachik regional zone of areal volcanism with an area of 875 km^2, the southern part of which is called Tolbachik Dol. Mineralogically, the most interesting active fumaroles are located in the apical part of the Second scoria cone of the Northern Breakthrough of the Great Tolbachik Fissure Eruption (NB GFTE)of 1975–1976. This cone, which is located 18 km south of Plosky Tolbachik and has a height of ~300 m, is a monogenic volcano that arose in 1975 (The Great ..., 1984). It still exhibits fumarolic activity: numerous gas outlets, the temperature of which reaches 500°C according to our measurements in 2012–2021, are observed on the surface here.

The fumaroles of the second cone of the NB GFTE are of oxidative type. Due to the high permeability of slag structures, volcanic gas in them mixes with atmospheric oxygen even before the onset of exhalation mineral formation, and so the mineralization formed in fumaroles is represented mainly by various oxygen compounds and, to a lesser extent, by fluorides and chlorides. In the fumaroles of Tolbachik, about three-and-a-half-hundred mineral species, over a third of which are new and mostly unknown minerals in other geological formations, were reliably identified to date. Representatives of more common mineral species, which are also found in other settings, are often characterized here by unusual sets of impurities and peculiar patterns of isomorphic substitutions. The main geochemical factor that determined the mineral diversity and mineralogical uniqueness of the Tolbachik fumarole systems was the enrichment of exhalations in chalcophile elements—Cu, Zn, Pb, Sn, As, Se, Tl, etc.—which allowed the formation of ore mineralization that is atypical for fumaroles of the vast majority of other volcanoes (Vergasova and Filatov, 1993; Pekov et al., 2020).

Sulphates of the langbeinite group that are represented by members of the langbeinite–calciolangbeinite series and vanthoffite are found in incrustations of several active fumaroles of the second cone of the NB GFTE. Most of them are concentrated in three fumaroles: Arsenatnaya, Yadovitaya, and Main Tenoritovaya.

The Arsenatnaya fumarole contains both langbeinite and two polymorphs of calciolangbeinite. Detailed information on the zonal distribution of exhalation mineral assemblages in the section of this fumarole is given in (Pekov et al., 2018a; Shchipalkina et al., 2020). Langbeinite–calciolangbeinite mineralization is developed in the middle (along the section) part of the fumarole, in the so-called "sulfate and polymineral zones," where the temperature that we measured in different areas varies in the range of 180–400°C. In the highest temperature of these chambers, in incrustations consisting mainly of arsenates (mainly johillerite, calciojohillerite, badalovite, nikenichite, tilazite, and svabite), anhydrite, sulfates of the aphthitalite group, As-enriched sanidine, fluorophlogopite, hematite, sometimes cristobalite or tridymite, and calciolangbeinite, including rhombic, usually in small quantities, mainly occurs. Above, in associations where, besides the above minerals, a variety of purely

copper arsenates (lammerite, lammerite-β, kozyrevskite, eriklaxmannite, and popovite), urusovite and bradachekite, as well as tenorite, are widely developed, one of the leading minerals in incrustations is calciolangbeinite-*C*, as well as, especially, langbeinite. Even higher in the section, in cavities with various copper sulfates and oxosulfates (fedotovite, piipite, wulffite, etc.), calciolangbeinite is noticeably less common, while langbeinite is very abundant. Vanthoffite in the Arsenatnaya fumarole occurs in the same zones as langbeinite in association with it, as well as with krashinnikovite, euchlorine, fedotovite, piypite, wulffite, anglesite, tenorite, hematite, silica phases, sanidine, and sellaite, as well as, sometimes, with sylvin, halite, and fluorophlogopite.

In the incrustations of the Yadovitaya fumarole, the most detailed description of which is given in (Vergasova and Filatov, 2016), langbeinite and calciolangbeinite-*C* are closely associated with sanidine, fedotovite, euchlorine, piypite, parawulffite, chlorothionite, palmierite, saranchinaite, lammerite, lionsite, pseudobrookite, tenorite, and hematite. Calciolangbeinite-*O* was not detected here. Vanthoffite was noted together with langbeinite, euchlorine, wulffite, chlorothionite, and tenorite.

In the Main Tenorite fumarole, langbeinite and vanthoffite are observed in close intergrowths with each other, as well as with kononovite, anglesite, sylvite, halite, and tenorite. Calciolangbainite was not found in the incrustations of this fumarole.

Crystals of langbeinite and calciolangbeinite-*C* from fumarolic exhalations usually have a tetrahedral or, being formed by uniformly developed faces of the {111} and {1-11} tetrahedra, pseudo-octahedral habit. Sometimes, they have weakly developed faces of cube {100} and/or rhombic dodecahedron {110}.

Langbeinite is characterized by well-formed colorless water-transparent crystals with a size of no larger than 0.7 mm (usually, <0.2 mm), which grow on calciolangbeinite-*C* segregations or form small (up to 1–2 cm^2 in area) brushes on altered basalt slag (Figs. 1a, 2a, 2b). There are split individuals to varying degrees: from block crystals with mosaic faces to spherocrystals are often observed (Figs. 2c, 2d). Sometimes, langbeinite forms clear-crystalline or glassy crusts with a thickness of up to 1–2 mm. Langbeinite "bubbles," which are hollow formations of a spherical or irregular shape with brittle walls made of a porous fine-crystalline aggregate of langbeinite, were found in fumarole chambers with copper sulfates. They reach 6 cm in the cross section. In the Main Tenoritovaya fumarole, langbeinite is sometimes observed as creamy brownish "buds" consisting of strongly split (?) tabular crystals (Fig. 3), which is uncharacteristic of this sulfate in other fumaroles. We believe that these are pseudomorphoses of langbeinite over vanthoffite.

Calciolangbeinite-*C* is observed in fumarolic incrustations in the form of colorless, snow-white, light gray, pale or deep pink, yellow, reddish, and pale brown crystals or irregularly shaped grains with a size of up to 2 mm. They form cluster-shaped aggregates and brushes with an area of up to several tens of square centimeters, covering altered basalt slag or segregations of earlier exhalation minerals (Figs. 1b, 1c). Calciolangbeinite-*C* crystals are characterized by "worn," rounded edges, as well as a cavernous or mosaic surface of the faces (Fig. 2e), while well-faceted individuals are very rare. There are distorted (flattened and elongated), as well as skeletal (rib and vertex), crystals (Fig. 1d). This sulfate often forms massive crusts with a thickness of up to 2 mm (Figs. 2a, 2b), as well as fine-grained "blotches" with a thickness of several microns on the surface of other minerals.

Calciolangbeinite-*O* was not found in the form of crystals (Pekov et al., 2022). It is characterized by massive colorless, grayish, or yellowish crusts with a thickness of up to 0.5 mm (Figs. 2f, 4d).

Joint aggregates of langbeinite and calciolangbeinite-*C* that consist of individuals of several generations are widespread in the Arsenatnaya and Yadovitaya fumaroles.

Calciolangbeinite-*C* often overgrows earlier segregations of langbeinite (Figs. 4a, 4c), being at the same time a substrate for its late nucleation crystals (Fig. 2e). Zoned crystals, in which a regular successive change of the Ca-dominant member of the series by the Mg-dominant one, or vice versa, would be traced, are not typical for these sulfates, but zones of different composition are sometimes very clearly manifested in individual crystals of langbeinite.

Sometimes, in individuals of calciolangbeinite, decomposition structures are observed, which are very small (a few microns in size) subindividuals of langbeinite in a matrix of calciolangbeinite-*C* (identification of these phases was carried out by Raman spectroscopy, see below) (Figs. 4a, 4b).

Vanthoffite in fumarolic incrustations is most often observed in the form of crusts consisting of small (up to 0.3 mm), usually split, lamellar, or tabular crystals collected in "buds" 0.5–1 mm in size (Figs. 5a, 5b, 5d).

Somewhat distorted, sometimes saddle-shaped, pseudorhombohedral crystals are encountered (Fig. 5c), the size of which does not exceed 0.2 mm. The secretions of this sulfate are colorless or milky white, brownish yellow, or light coffee in color.

CHEMICAL COMPOSITION

Data on the chemical composition of sulfates were obtained at the Laboratory of Local Methods for Studying Substances, Faculty of Petrology, Moscow State University, using scanning JEOL JSM-6480LV and Superprobe JXA-8230 electron microscopes equipped with energy-dispersive spectrometers. Analyses were performed at an accelerating voltage of 20 kV and a probe current of 7 nA. The following standards

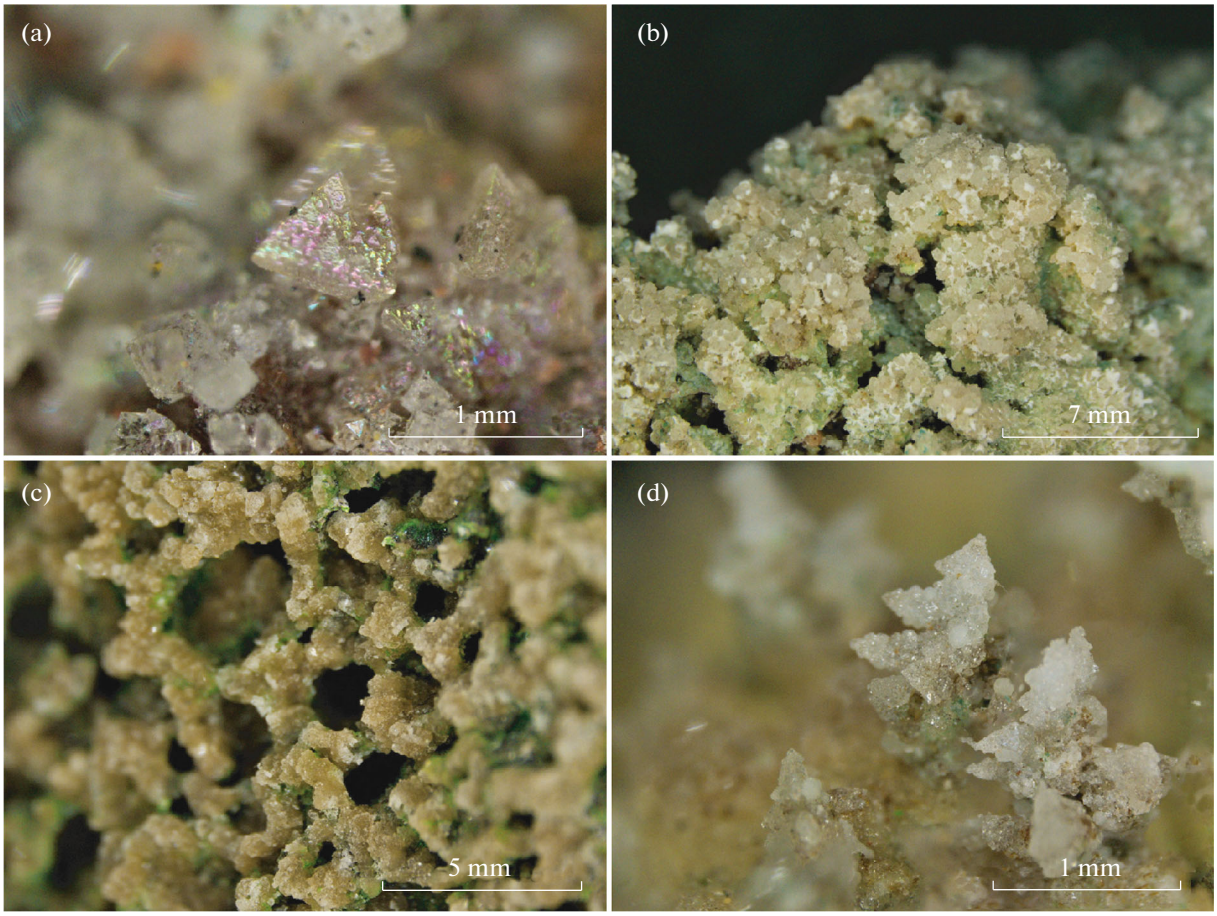

Fig. 1. Langbeinite-group minerals in fumarolic incrustations of the Tolbachik volcano: (a) tetrahedral crystals of langbeinite growing on altered basalt scoria, (b) brush of calciolangbeinite-*C* crystals with ingrowths of bluish-green alarsite and yellow-green kozyrevskite, (c) brush of calciolangbeinite-*C* crystals with ingrowths of green piypite, and (d) skeletal crystals of calciolangbeinite-*C* (vertex-developed form) each "branch" of which is overgrown with skeletal crystals of langbeinite (edge-developed form).

were used: K, microcline; Na, albite; Rb, $Rb_2Nb_4O_{11}$; Cs, $Cs_2Nb_4O_{11}$; Mg, diopside; Ca, $CaSiO_3$; Fe, FeS_2; Mn, $MnTiO_3$; Cu, Cu; Zn, gahnite; Cd, CdS; Al, jadeite; S, $SrSO_4$. The contents of other elements with atomic numbers >8, as well as N, turned out to be below the limits of detection by the electron probe-method.

Empirical formulas of minerals of the langbeinite group are given per 12 oxygen atoms, and those of the vanthoffite group are given per 16 oxygen atoms.

When calculating the empirical formulas of langbeinite and calciolangbeinite, it was assumed that divalent cations, Al and Fe (according to the strongly oxidizing nature of the mineral formation medium, impurity iron is calculated as Fe^{3+}), occupy octahedral position *M* while Na preferentially enters position *A*. In this case, (1) in the case of an amount M^{2+} exceeding 2.00 apfu, excess Ca was placed in position *A* due to the largest Ca^{2+} radius among divalent cations, and (2) with a deficiency of divalent cations, the *M* position was supplemented with Na up to 2.00 apfu.

Representative samples of analyses of langbeinite and calciolangbeinite are presented in Tables 1 and 2, respectively.

As we showed earlier, langbeinite and calciolangbeinite from Tolbachik fumarolic exhalations are characterized by wide variations in the Ca : Mg ratio in octahedral sites. The fraction of Ca in the *A* position is usually small: it rarely exceeds 0.05 apfu and only in some cases reaches 0.2 and even 0.4 apfu (Pekov et al., 2022). The Ca amount in the octahedral position in langbeinite varies mainly within 0.00–0.4 apfu (Fig. 6). In the Ca-dominant part of the series, there was revealed a series of compositions from almost pure $K_2Ca_2(SO_4)_3$ (calciolangbeinite-*O*), in which the magnesium concentration is below the detection limit by the electron-probe method, to an intermediate member of the series with 50 mol % $K_2Mg_2(SO_4)_3$.

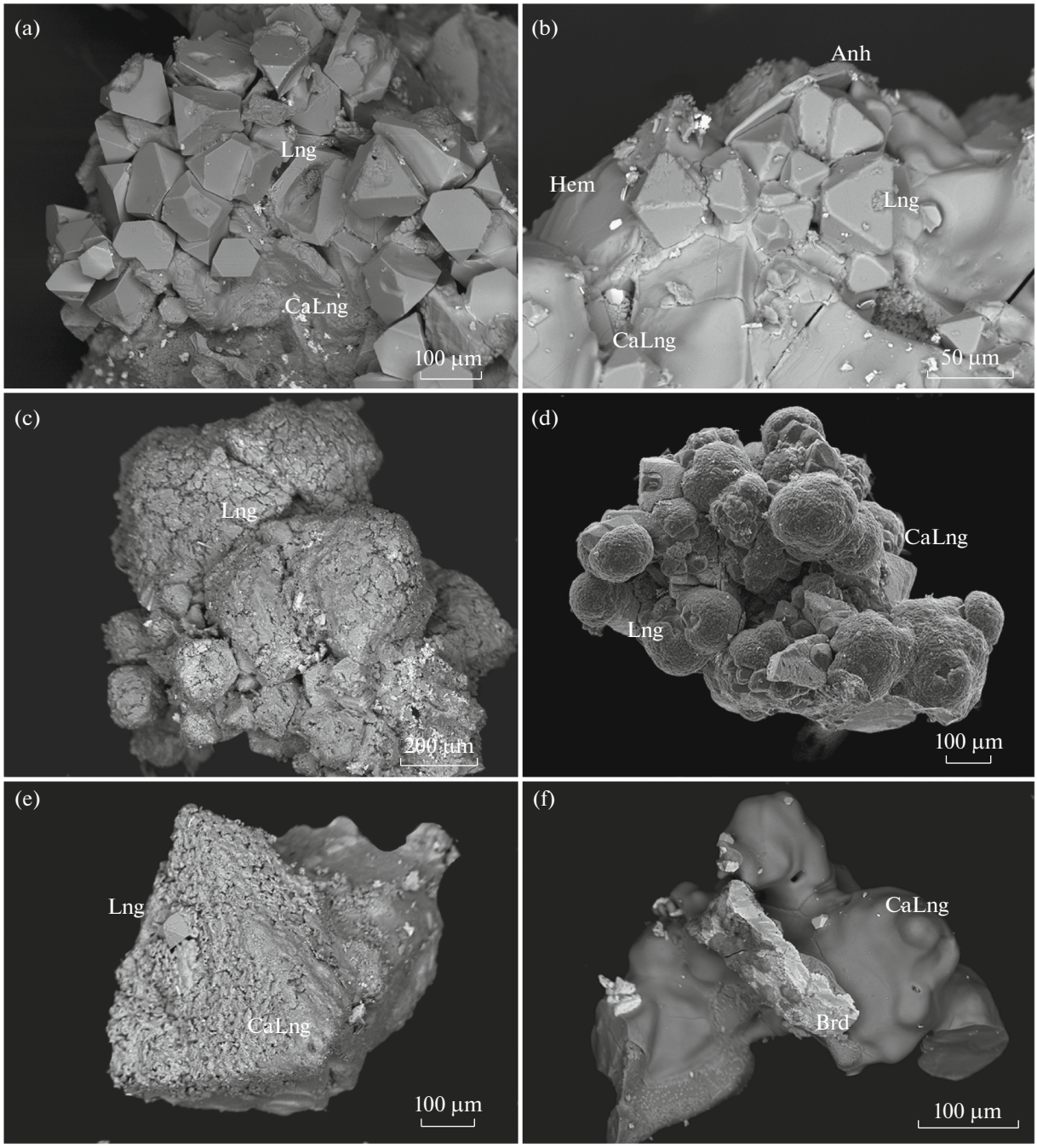

Fig. 2. Morphology of langbeinite-group minerals from fumarolic exhalations of the Tolbachik volcano: (a) tetrahedral crystals of langbeinite (Lng) overgrowing a massive crust of calciolangbeinite-*C* (CaLng), (b) pseudo-octahedral crystals of langbeinite on massive crust of calciolangbeinite-*C* with anhydrite (Anh) and hematite (Hem), (c) cluster of split langbeinite crystals, (d) aggregate of spherulites of langbeinite on calciolangbeinite-*C*, (e) tetrahedral calciolangbeinite-*C* crystal with mosaic face surface overgrowing by pseudo-octahedral langbeinite crystal, and (f) massive crust of calciolangbeinite-*O* with bradaczekite (Brd) and hematite. SEM (BSE) images.

However, most analyses lie in the region ($Ca_{1.2–2.0}$-$Mg_{0.8–0.0}$) (Fig. 6).

About a dozen analyses of calciolangbeinite with a content above 20 mol % $K_2Mg_2(SO_4)_3$ were obtained using a probe defocused to an area of 5 × 5 μm on samples with decay structures.

Besides Ca in langbeinite and Mg in calciolangbeinite, a number of other impurity elements were recorded in these minerals.

First of all, these are chalcophile elements: copper and zinc. Their highest concentrations are 0.53 apfu Zn (9.9 wt % ZnO) and 0.18 apfu Cu (3.3 wt % CuO),

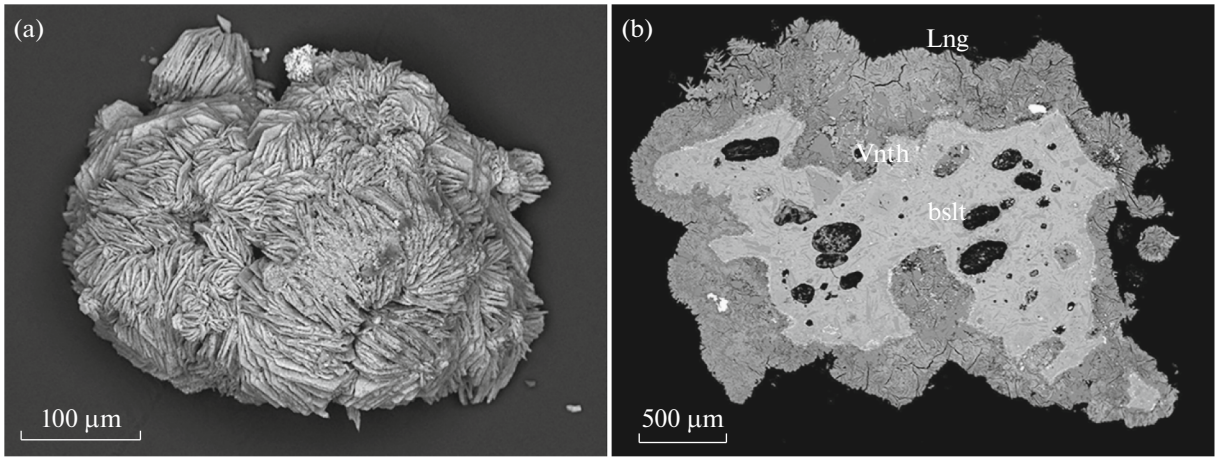

Fig. 3. Pseudomorphs of langbeinite after vanthoffite: (a) "kidney" consisting of split tabular vanthoffite crystals replaced by langbeinite; (b) polished section of a similar kidney: relics of vanthoffite (Vnth) in the langbeinite aggregate (Lng) with unaltered basalt (bslt) in the core of the kidney. SEM (BSE) images.

which are observed in almost calcium-free langbeinite (Figs. 6, 7) from association with copper sulfates. In the sample most enriched in these elements, the content of the end member $K_2(Zn, Cu)_2(SO_4)_3$ reaches 30 mol %. For both polymorphic modifications of calciolangbeinite, these impurities are less typical. The maximum total concentration of Zn and Cu recorded in calciolangbeinite-*C* is 0.25 apfu (2.8 wt % CuO and 1.5 wt % ZnO), but, in most of the studied samples, it does not exceed 0.1 apfu or is completely below the limit of detection by the electron probe method.

In one of the samples of calciolangbeinite-*C*, cadmium was noted in an amount of 0.02 apfu Cd (0.7 wt % of CdO).

A small amount of manganese is usually present (up to 0.05 apfu Mn = 1.0 wt % MnO), iron (up to 0.05 apfu Fe^{3+} = 1.8 wt % Fe_2O_3), and aluminum (no more than 0.01 apfu Al = 0.1 wt % Al_2O_3).

Monovalent cations, in addition to the species-forming potassium, are represented in the minerals of the langbeinite group by sodium (up to 0.31 apfu Na = 2.3 wt % Na_2O) and rubidium (up to 0.06 apfu Rb = 1.3 wt % Rb_2O). In cadmium-enriched calciolangbeinite-*C*, cesium was also detected in an amount of 0.01 apfu Cs = 0.4 wt % Cs_2O. It should be noted that, in the electron-probe analysis of langbeinite samples with a high Zn concentration, as a result of the superposition of the analytical lines *K*α Na and *K*α Zn, the Na amount turned out to be overestimated; 10 wt % ZnO accounts for ~1 wt % "fictitious" Na_2O.

Vanthoffite from Tolbachik exhalations is characterized by impurities of Zn, Cu, Mn, Fe, Ca, and K (Table 3). Their noted highest concentrations are as follows: Zn, 0.14 apfu = 2.0 wt % ZnO; Cu, 0.12 apfu = 1.7 wt % CuO; Mn, 0.09 apfu = 1.2 wt % MnO; Fe, 0.02 apfu = 0.5 wt % Fe_2O_3; Ca, 0.04 apfu = 0.4 wt % CaO; and K, 0.06 apfu = 0.6 wt % K_2O.

Some sodium deficiency observed in the analyses of our vanthoffite relative to the ideal content of large cations Na + K + Ca = 6 apfu (Table 3) is definitely associated with a small loss of this component during the electron-probe analysis, which is generally typical for such Na-rich compounds.

No components that could replace S^{6+} were found in the studied minerals.

RADIOGRAPHIC DATA

The samples were studied by powder X-ray diffractometry using a Rigaku R-AXIS Rapid II diffractometer with a cylindrical IP detector (monochromatized Co*K*α radiation, Debye–Scherrer geometry, and *d* = 127.4 mm). The integration of the initial data from the cylindrical detector was carried out using the osc2tab software package (Britvin et al., 2017).

The unit cell parameters calculated from powder X-ray diffraction patterns of langbeinite and calciolangbeinite-*C* of various compositions are given in Table 4.

For a sample of Tolbachik langbeinite with a minimal impurity content, parameter *a* and volume *V* of the unit cell are very close to those for the synthetic analog of langbeinite (*a* = 9.92 Å, *V* = 977 Å^3: Mereiter, 1979). At an increase in the $K_2Ca_2(SO_4)_3$ end-member content in the langbeinite–calciolangbeinite series, the values of *a* and *V* increase almost linearly (Fig. 8).

RAMAN SPECTROSCOPY

Raman spectra were recorded at the Faculty of Mineralogy of Moscow State University on an

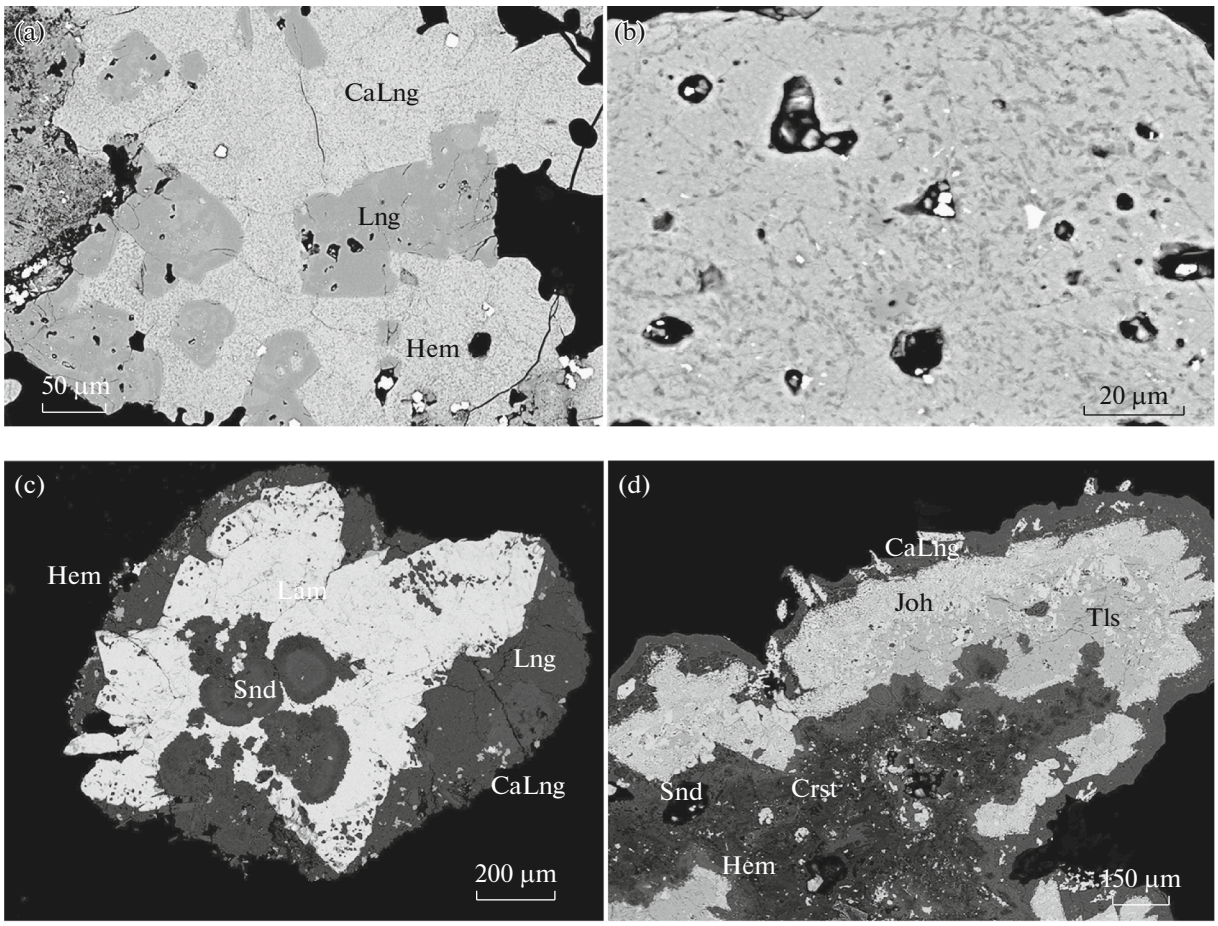

Fig. 4. Langbeinite-group minerals from fumarolic exhalations of the Tolbachik volcano: (a) langbeinite (Lng) crystals overgrown by calciolangbeinite (CaLng) with breakdown structures; (b) calciolangbeinite with breakdown structures; (c) crust of calciolangbeinite-*C* and langbeinite with hematite inclusions (Hem) covering aggregate of lammerite crystals (Lam) with inclusions of sanidine spherulites (Snd); and (d) calciolangbeinite-*O* crust on johillerite (Joh) and tilasite (Tls), which overgrow aggregate of sanidine and cristobalite (Crst). Polished sections. SEM (BSE) images.

EnSpectr R532 spectrometer (Russia) at a laser-radiation wavelength of 532 nm and an output beam power of 4 mW. The spectra were obtained on arbitrarily oriented samples in the range of 200–4000 cm^{-1} in the signal-accumulation mode for 1 s, with averaging over 50–70 exposures (the range up to 1500 cm^{-1} is shown in the figures since bands above the background level are further not observed). The focal beam diameter was 10 μm.

In the Raman spectra of both langbeinite and vanthoffite group minerals, bands with frequencies above 400 cm^{-1} correspond to vibrations of S-O bonds in tetrahedral sulfate groups (Latush et al., 1983; Nakamoto, 2009). Completely symmetric stretching vibrations ν_1 (A_1) correspond to intense bands in the range of 1000–1050 cm^{-1}, asymmetric stretching vibrations ν_3 (F_2) correspond to series of bands in the range of 1070–1300 cm^{-1}. The bending symmetric ν_2 (E) and asymmetric ν_4 (F_2) vibrations include bands in the ranges of 400–500 and 550–700 cm^{-1}, respectively. A weak band near 215 cm^{-1} in the vanthoffite spectrum belongs to *Me*···O bond vibrations or lattice acoustic modes.

Raman spectra of artificial analogues of manganolangbeinite $K_2Mn_2(SO_4)_3$ (Latush et al., 1983) and efremovite (Košek et al., 2018); synthetic langbeinite-like sulfates with compositions $Tl_2Cd_2(SO_4)_3$, $Rb_2Cd_2(SO_4)_3$, and $(NH_4)_2Cd_2(SO_4)_3$ (Latush et al., 1983); and members of artificially obtained series $K_2Mg_2(SO_4)_3$–$Na_{1.9}K_{0.1}Mg_2(SO_4)_3$ (Trussov et al., 2019), as well as natural ferrorefremovite (Kasatkin et al., 2021), were earlier considered in the literature. In our study (Pekov et al., 2022), Raman spectra of calciolangbeinite-*O* from Tolbachik fumarolic exhalations and pyrometamorphic rocks of the Hatrurim complex (Israel), as well as calciolangbeinite-*C* from Tolbachik and langbeinite from evaporites of the Stebnik potassium salt deposit (Ukraine), are provided. In this paper, we present the results of subsequent, more detailed spectroscopic studies of a series of Tolbachik

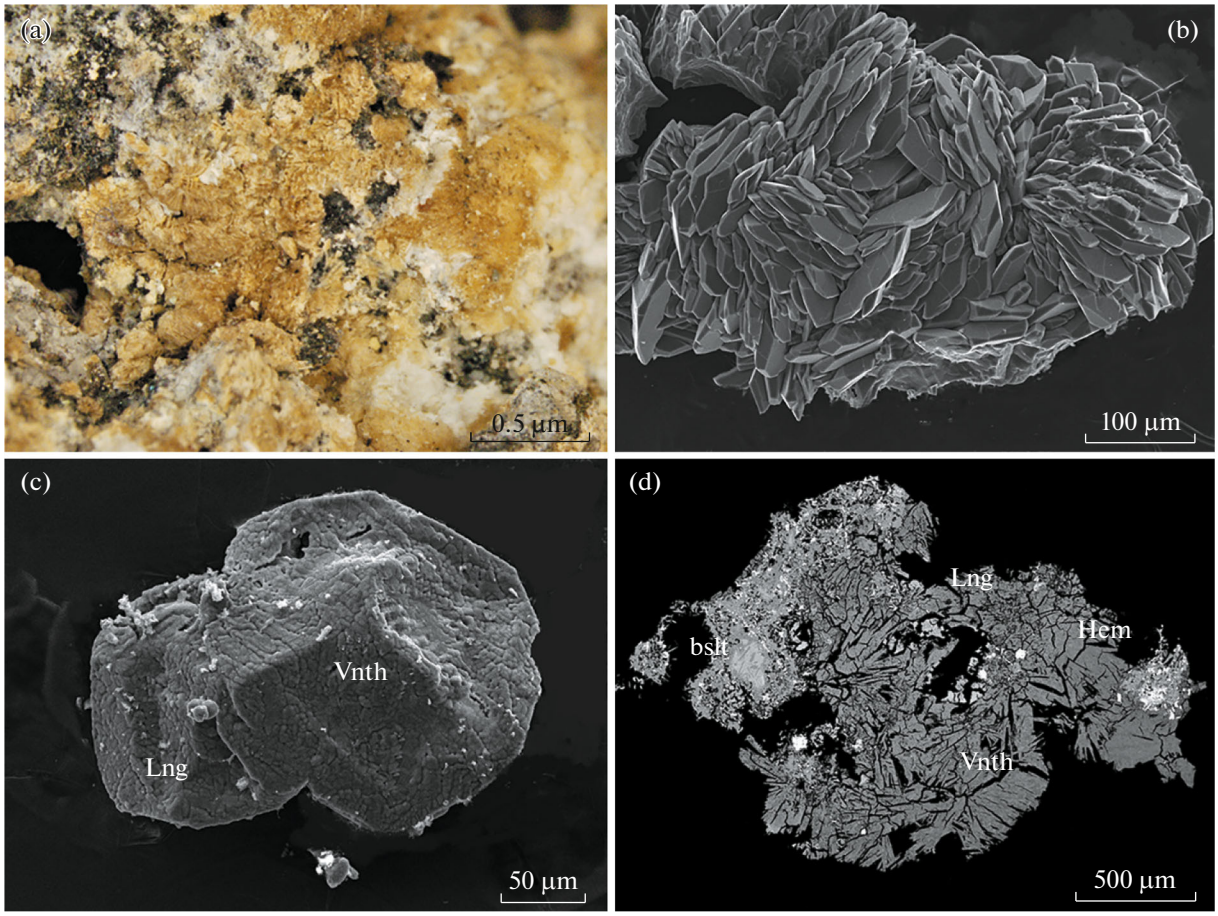

Fig. 5. Vanthoffite from fumarolic exhalations of the Tolbachik volcano: (a) light brown crust of tabular vanthoffite crystals overgrowing aggregate of white langbeinite on basalt scoria, (b) cluster of tabular vanthoffite crystals, (c) cluster of pseudorhombohedral distorted vanthoffite crystals (Vnth) with small spherulites of langbeinite (Lng), and (d) aggregate of vanthoffite crystals on altered basalt scoria (bslt) with overgrowing langbeinite and hematite (Hem) (polished section). (b–d) REM images ((b) SE; (c, d) BSE).

samples for langbeinite-group minerals of various chemical compositions.

Differences in the Raman spectra of langbeinite (Fig. 9) and both modifications of calciolangbeinite (Fig. 10) are expressed primarily in the position and shape of the band of symmetric stretching vibrations ν_1. In the spectrum of high-magnesian langbeinite with a minimal amount of impurities, as in the spectrum of langbeinite from Stebnik, it is narrow and symmetrical, with a maximum at 1053–1054 cm^{-1}. The spectra of samples enriched in elements heavier than Mg–Ca, Zn, and/or Cu show a slight asymmetry of this band, as well as a slight shift toward lower frequencies, no far than 1047 cm^{-1}. In calciolangbeinite-*C*, the band of symmetric stretching vibrations is in the range of 1034–1025 cm^{-1} (with an increase in the amount of Ca, it also shifts towards low frequencies). It is asymmetric and has a distinct shoulder at 1005 cm^{-1}. In the spectra of samples containing less than 10 mol % of $K_2Mg_2(SO_4)_3$, this band is split into 1007- and 1025–1026-cm^{-1} components, while, at the lowest amount of the langbeinite end member (~5 mol % or less, i.e., for calciolangbeinite-*O*), it is represented by a doublet with components 994–1000 and 1011–1012 cm^{-1} that are complicated by a small shoulder at ~1021 cm^{-1}.

The marked decrease in the frequencies of the bands corresponding to symmetric stretching vibrations at an increase in the concentration of Ca, Zn, and Cu is natural and is due to the higher atomic mass of these elements compared to Mg. The asymmetry of the ν_1 band in langbeinite and calciolangbeinite-*C* with various combinations of cations is associated with a decrease in the local symmetry of the medium around tetrahedral sulfate groups when different types of cations are involved in the S–O bond vibrations. The clearly pronounced splitting of this band in low-Mg samples of calciolangbeinite is caused by a general decrease in the symmetry of the structure upon transition from the cubic to rhombic modification. The appearance of a doublet in the region of symmetric

Table 2. Chemical composition of calciolangbeinite-*C* and calciolangbeinite-*O* from fumarolic exhalations of the Tolbachik volcano

	1	2	3	4	5	6	7	8	9	10	11	12
						wt %						
Na_2O	0.35	0.36	1.06		0.71	0.53	0.21	0.20	0.62	0.43	0.40	
K_2O	20.50	19.10	20.46	21.03	21.21	19.71	20.73	21.62	20.71	21.08	20.97	21.71
Rb_2O	0.47	0.44	0.53	0.65	0.26	1.27	0.47	0.57	0.42	0.57	0.33	0.26
Cs_2O						0.40						
MgO		0.92	1.92	2.25	2.73	3.41	3.45	3.73	3.78	4.17	6.17	8.20
CaO	24.30	24.56	21.05	21.27	19.65	18.88	18.11	19.32	18.81	17.38	16.29	11.87
MnO				0.13	0.26		0.34		0.24	0.27		0.23
CuO							1.68		0.25	0.51		0.40
ZnO						0.57	0.31		0.97			0.93
CdO						0.68						
Fe_2O_3										0.37		
SO_3	53.07	54.25	53.68	54.77	54.24	53.62	53.16	54.92	54.86	54.95	54.19	54.00
Sum	98.69	98.63	98.70	100.10	99.06	99.07	98.46	100.36	100.68	99.73	98.56	97.59
	Formula coefficients per 12 O atoms											
K	1.97	1.80	1.95	1.97	2.01	1.88	1.99	2.02	1.93	1.98	1.98	2.06
Na	0.01	0.05	0.05			0.02	0.02		0.05		0.03	
Rb	0.02	0.02	0.03	0.03	0.01	0.06	0.02	0.03	0.02	0.03	0.02	0.01
Ca		0.04										
Cs						0.01						
$\sum A$	2.00	1.91	2.03	2.00	2.02	1.97	2.03	2.05	2.00	2.01	2.03	2.07
Na	0.04		0.10		0.10	0.06	0.01	0.03	0.04	0.06	0.03	
Mg		0.10	0.21	0.25	0.30	0.38	0.39	0.41	0.41	0.46	0.68	0.91
Ca	1.96	1.90	1.69	1.68	1.56	1.51	1.46	1.51	1.47	1.37	1.29	0.94
Mn				0.01	0.02		0.02		0.02	0.02		0.01
Cu							0.10		0.01	0.03		0.02
Zn						0.03	0.02		0.05			0.05
Cd						0.02						
Fe										0.01		
$\sum M$	2.00	2.00	2.00	1.94	1.98	2.00	2.00	1.95	2.00	1.95	2.00	1.93
$\sum Me$	4.00	3.91	4.03	3.94	4.00	3.97	4.03	4.00	4.00	3.95	4.03	4.00
S^{6+}	3.00	3.01	3.01	3.02	3.02	3.01	3.00	3.01	3.01	3.03	3.00	3.01

ΣM = Mg + Ca + ^{M}Na + Mn + Cu + Zn + Cd + Fe; ΣA = K + ^{A}Na + Rb + ^{A}Ca; ΣMe is the sum of all metals. An empty cell indicates the content of the component below the detection limit. an. 1–4, 6, 7, 10, 11, Arsenatnaya fumarole; an. 5, 8, 9, 12, Yadovitaya fumarole.

stretching vibrations in orthorhombic phases instead of a single band in cubic modifications was observed earlier and in the Raman spectroscopic study of phase transitions in a number of synthetic langbeinite-like sulfates (Latush et al., 1983).

Some differences are also noted in the regions corresponding to S–O bending vibrations. Asymmetric deformation vibrations (ν_4) at 550–700 cm^{-1} in the spectrum of pure magnesian langbeinite produce a distinct triplet. As is seen in Fig. 9, when any isomorphic impurities appear in the mineral, the configuration of the spectrum changes. For calciolangbeinite-*C*, the ν_4 band is narrower, and it is split only in samples with a low (~10 mol %) content of the $K_2Mg_2(SO_4)_3$ end member. In the spectra of calciolangbeinite-*O*, band splitting is manifested in the region of both asymmetric and symmetric deformation vibrations.

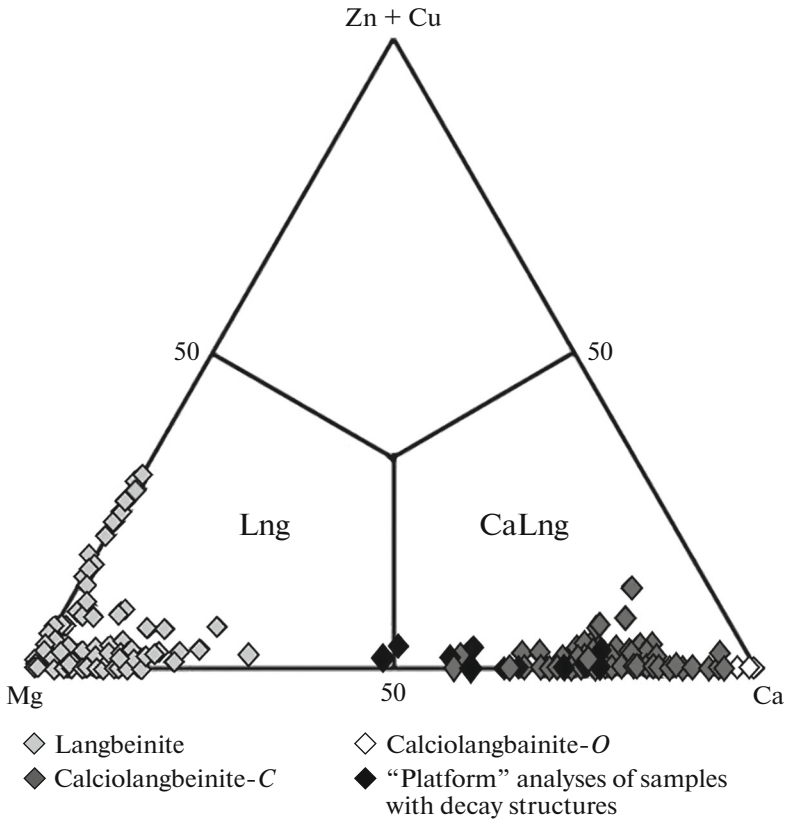

Fig. 6. Ratios of Mg, Ca and chalcophile Zn + Cu in langbeinite-group minerals from fumarolic exhalations of the Tolbachik volcano, Kamchatka.

The Raman spectra of samples with decomposition structures (Fig. 11) show two bands in the region of symmetric stretching vibrations: at 1052 cm^{-1}, which is characteristic of langbeinite, and at 1026 cm^{-1}, which is related to cubic calciolangbeinite. Hence, we can conclude that the decomposition products of high-magnesian calciolangbeinite are represented by langbeinite and calciolangbeinite-*C*.

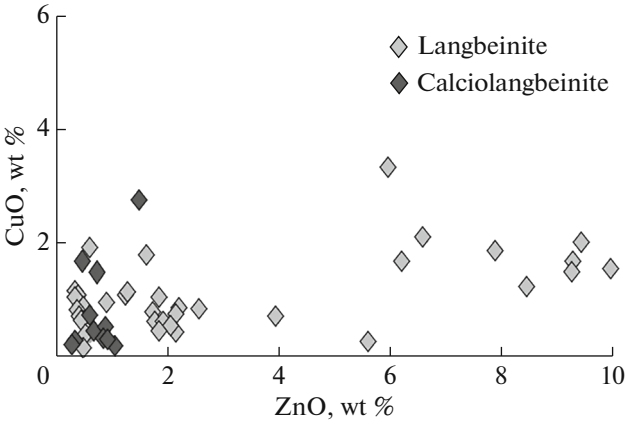

Fig. 7. Ratios of admixed copper and zinc in langbeinite-group minerals from fumarolic exhalations of the Tolbachik volcano, Kamchatka.

No data on Raman spectroscopy of vanthoffite could be found in the literature, and we are publishing the Raman spectrum of this mineral for the first time. In the spectrum of the Tolbachik vanthoffite (Fig. 12), completely symmetrical (ν_1) S–O stretching vibrations produce a doublet with components at 1005 and 1016 cm^{-1}. In the regions of symmetric (ν_2) (440–500 cm^{-1}) and asymmetric (ν4) (600–660 cm^{-1}) bending vibrations, the bands are also split, which is due to the above-discussed presence in the structure of this mineral of two sorts of sulfate tetrahedra located in heterogeneous layers (see (Balić-Žunić et al., 2020)).

DISCUSSION

As our data show, unlike their almost chemically pure analogs from the evaporite deposits, the minerals of the langbeinite and vanthoffite group from the fumarole exhalations of the Tolbachik volcano are characterized by wide variations in the cationic composition, which are associated with the presence of various isomorphic impurities in positions *M* (mostly) and *A*.

The predominant number of Tolbachik samples of minerals of the langbeinite group according to the ratio of Ca and Mg belongs to the composition ranges

Table 3. Chemical composition of vanthoffite from fumarolic exhalations of the Tolbachik volcano

	1	2	3	4	5	6	7*
				wt %			
Na_2O	32.72	32.65	33.38	31.13	30.24	30.72	30.53
K_2O	0.08	0.33	0.10		0.28	0.20	
MgO	7.44	6.57	6.95	6.58	6.03	6.57	4.66
CaO	0.17	0.22					0.19
MnO		0.61		0.28	0.33	0.41	0.19
CuO				0.27	0.65	1.71	4.42
ZnO		0.42	1.03	1.57	2.01		2.03
Fe_2O_3				0.51			
SO_3	60.41	60.83	60.66	59.47	59.32	58.67	56.86
Total	100.82	101.63	102.12	99.81	98.86	98.28	98.88
				Formula coefficients per 16 O atoms			
K	0.01	0.04	0.01		0.03	0.02	
Na	5.67	5.64	5.75	5.50	5.38	5.49	5.57
Ca	0.02	0.02					0.02
Mg	0.99	0.87	0.92	0.89	0.83	0.90	0.65
Mn		0.05		0.02	0.03		0.02
Cu				0.02	0.05	0.12	0.31
Zn		0.03	0.07	0.11	0.14		0.14
Fe^{3+}				0.02			
$\sum M$	0.99	0.95	0.99	1.06	1.05	1.02	1.12
$\sum Me$	6.69	6.65	6.75	6.56	6.46	6.53	6.71
S^{6+}	4.05	4.07	4.04	4.06	4.09	4.06	4.02

* Analysis from (Shchipalkina et al., 2021). ΣM = Mg + Mn + Cu + Zn + Fe. $\Sigma Me = \Sigma M$ + Na + K + Ca. An empty cell indicates the content of the component below the detection limit. an. 1, 4, 7, Arsenatnaya fumarole; an. 2, 3, 5, Main Tenoritovaya fumarole; an. 6, Yadovitaya fumarole.

($Mg_{2.0–1.6}Ca_{0.0–0.4}$) for langbeinite and ($Ca_{1.2–2.0}Mg_{0.8–0.0}$) for calciolangbeinite. The formation of a solid solution between the magnesian and calcium members of the group was obviously facilitated by high crystallization temperatures in fumarole cavities: based on the geothermometry data (Pekov et al., 2018a; Shchipalkina et al., 2021) and the results of our temperature measurements, we can assume that langbeinite and calciolangbeinite with wide variations in the Ca : Mg ratio were formed mainly at temperatures no lower than 400°C. The isomorphism between Ca^{2+} and Mg^{2+} in these sulfates, however, turned out to be limited under these conditions, which is definitely caused by a significant difference in the radii of these cations (in octahedral coordination, 0.72 Å for Mg and 1.00 Å for Ca (Shannon, 1976)). The actual crystal chemical aspect of the series of langbeinite–calciolangbeinite solid solutions was discussed in detail in our previous study (Pekov et al., 2022). Therefore, we will dwell in more detail on the decomposition phenomena in the intermediate members of the series, which was not previously known.

Compositionally different members of the $K_2Mg_2(SO_4)_3$–$K_2Ca_2(SO_4)_3$ solid solution with the langbeinite structure were repeatedly obtained artificially (Ramsdell, 1935; Morey et al., 1964; Rowe et al., 1967). To do this, powders of simple sulfates K, Mg, and Ca mixed in various proportions in accordance with the specified composition of the synthesized sulfate were melted at temperatures above 870°C and then cooled rapidly, which led to quenching of crystallization products (Morey et al., 1964). According to the results of thermodynamic modeling and experimental data, continuous solid solution $K_2Mg_2(SO_4)_3$–$K_2Ca_2(SO_4)_3$ is stable over a wide temperature range up to the melting point, which varies depending on the ratios of the components in the system (Tesfaye et al., 2020; Yazhenskikh et al., 2021). However, the lower limit of its stability was not determined experimentally, and the possibility of decomposition upon cooling was not considered. For samples from Tolbachik's

Table 4. (2–9) Unit cell parameters of langbeinite and calciolangbeinite-*C* with different composition from the Tolbachik volcano in comparison with (1) data for a synthetic analogue of langbeinite

No.	Empirical formula	*a*, Å	*V*, Å^3
	Langbeinite, $P2_13$, $Z = 4$		
1	$K_2Mg_2(SO_4)_3$ (Mereiter, 1979)	9.92	977
2	$(K_{2.00}Rb_{0.01})_{\Sigma 2.01}(Mg_{1.92}Na_{0.06}Ca_{0.01})_{\Sigma 1.99}S_{3.01}O_{12}$	9.9320(2)	979.75(7)
3	$(K_{1.95}Na_{0.04}Rb_{0.01})_{\Sigma 2.00}(Mg_{1.68}Ca_{0.23}Cu_{0.04}Mn_{0.02}Na_{0.02}Fe_{0.01})_{\Sigma 2.00}S_{3.00}O_{12}$	9.976(2)	992.7(5)
4	$(K_{1.84}Na_{0.04}Ca_{0.01}Rb_{0.01})_{\Sigma 1.90}(Mg_{1.54}Ca_{0.38}Cu_{0.03}Mn_{0.02}Zn_{0.02})_{\Sigma 1.99}S_{3.01}O_{12}$	10.01(6)	1003.5(5)
5	$(K_{1.79}Na_{0.22})_{\Sigma 2.01}(Mg_{1.83}Na_{0.09}Zn_{0.07}Ca_{0.01})_{\Sigma 2.00}S_{3.02}O_{12}$	9.887(1)	966.4(2)
6	$(K_{1.71}Na_{0.22}Rb_{0.04}Ca_{0.02})_{\Sigma 1.99}(Mg_{1.45}Zn_{0.45}Cu_{0.08}Mn_{0.03})_{\Sigma 1.99}S_{3.01}O_{12}$	9.90(1)	970.6(7)
	Calciolangbainite-*C*, $P2_13$, $Z = 4$		
7	$K_{2.01}(Ca_{1.24}Mg_{0.70}Na_{0.05}Mn_{0.02}Fe_{0.01}Al_{0.01})_{\Sigma 2.03}S_{3.00}O_{12}$ (Pekov et al., 2012)	10.1887(4)	1057.68(4)
8	$(K_{1.98}Rb_{0.02})_{\Sigma 2.00}(Ca_{1.44}Mg_{0.45}Na_{0.06}Mn_{0.02})_{\Sigma 1.97}S_{3.02}O_{12}$	10.21(1)	1063(3)
9	$(K_{1.97}Na_{0.01}Rb_{0.01})_{\Sigma 1.99}(Ca_{1.51}Mg_{0.35}Na_{0.09}Zn_{0.03}Mn_{0.01}Cu_{0.01})_{\Sigma 2.00}S_{3.02}O_{12}$	10.23(1)	1071.5(7)

fumaroles, the compositions of the initial phase that are estimated in the regions with decay structures using a defocused electron beam correspond to the region of magnesium-enriched calciolangbeinite ($Ca_{1.0–1.6}Mg_{1.0–0.4}$); one analysis formally refers to high-calcium langbeinite (Fig. 6). Formed at sufficiently high temperatures (probably over 400°C), these representatives of the series turned out to be unstable with decreasing temperature and decomposed into langbeinite and calciolangbeinite-*C* with a low Mg content. At the same time, in other, and rather numerous, samples of calciolangbeinite belonging to the same range of compositions, signs of decay are not observed. Apparently, these differences are associated with the rate of cooling of the samples: the decomposition of the solid solution occurs during the slow cooling of the incrustations in the fumarole cavities, while the quenching effect is triggered when the samples are quickly removed from the hot chambers.

A striking common feature of Tolbachin langbeinite, calciolangbeinite, and vanthoffite is the presence of significant amounts of impurity chalcophile elements, primarily Cu and Zn, which were not observed in these sulfates from other objects.

Zinc is preferentially concentrated in almost calcium-free langbeinite, while this element is present in a much smaller amount in calciolangbeinite (Figs. 6, 7). This fact is probably due to the fact that Zn^{2+} is much closer in ionic radius to Mg^{2+} than to Ca^{2+} (the ionic radii of these elements in octahedral coordination are 0.74, 0.72, and 1.00 Å, respectively (Shannon,

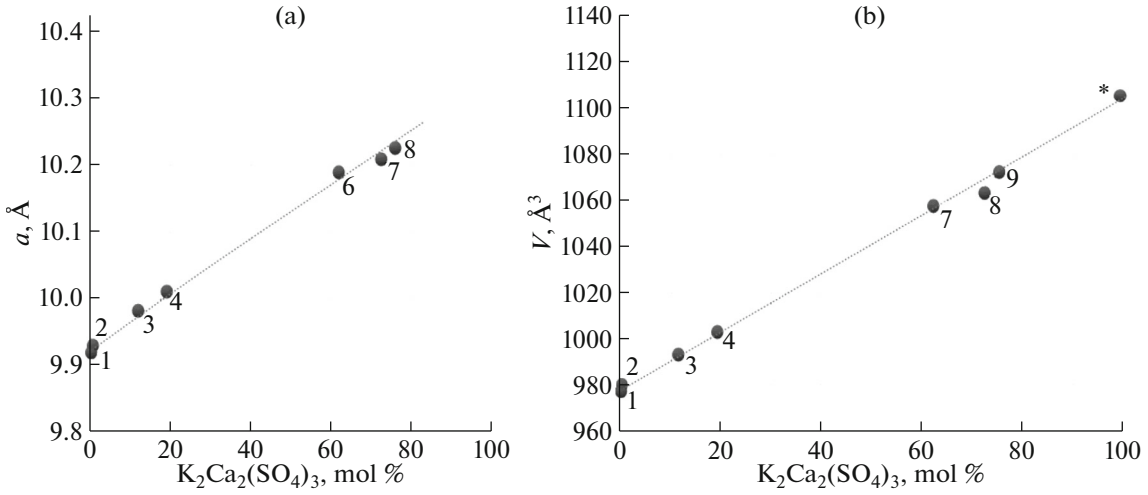

Fig. 8. Dependence of (a) parameter *a* and (b) cubic unit-cell volume *V* on the $K_2Ca_2(SO_4)_3$ content for members of the langbeinite-calciolangbeinite series. Numbers correspond to Table 4. * the orthorhombic unit-cell volume of calciolangbeinite-*O* (Pekov et al., 2022).

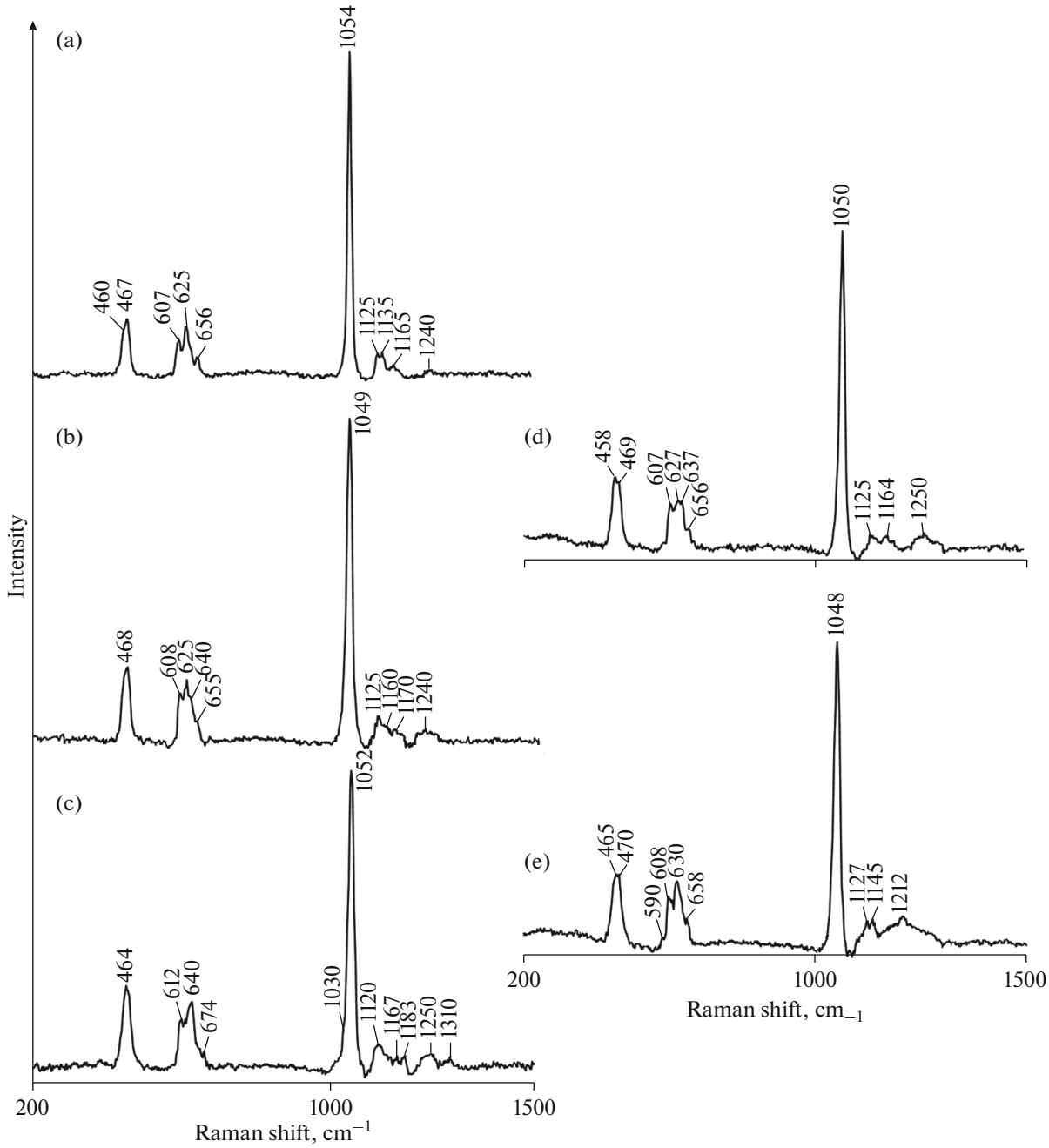

Fig. 9. Raman spectra of langbeinite with various compositions from fumarolic exhalations of the Tolbachik volcano (Kamchatka, Russia).

1976)). Note that the synthetic zinc analog of langbeinite $K_2Zn_2(SO_4)_3$ was known for a long time; single crystals of it were obtained by the Czochralski method from a melt (490°C) of simple sulfates (Speer and Salje, 1986). In Tolbachik vanthoffite, Zn^{2+} definitely replaces magnesium as well.

The highest recorded concentration of copper (3.3 wt % of CuO) in minerals of the langbeinite group is significantly lower than the maximal concentration of zinc (10.0 wt % of ZnO). Lander et al. (2017) note that attempts to synthesize a structural analog of langbeinite with $M = Cu^{2+}$ were unsuccessful. Rhombic phase $K_2Cu_2(SO_4)_3$ obtained instead of it that corresponds in stoichiometry to langbeinite-like compounds structurally differs significantly from them: Cu^{2+} cations in its structure center flat quadrangles and quadrangular pyramids rather than octahedrons. At temperatures above 400°C, this phase is replaced by the analogue of fedotovite $K_2Cu_3O(SO_4)_3$ (Lander et al., 2017). Significant isomorphism between Cu^{2+}

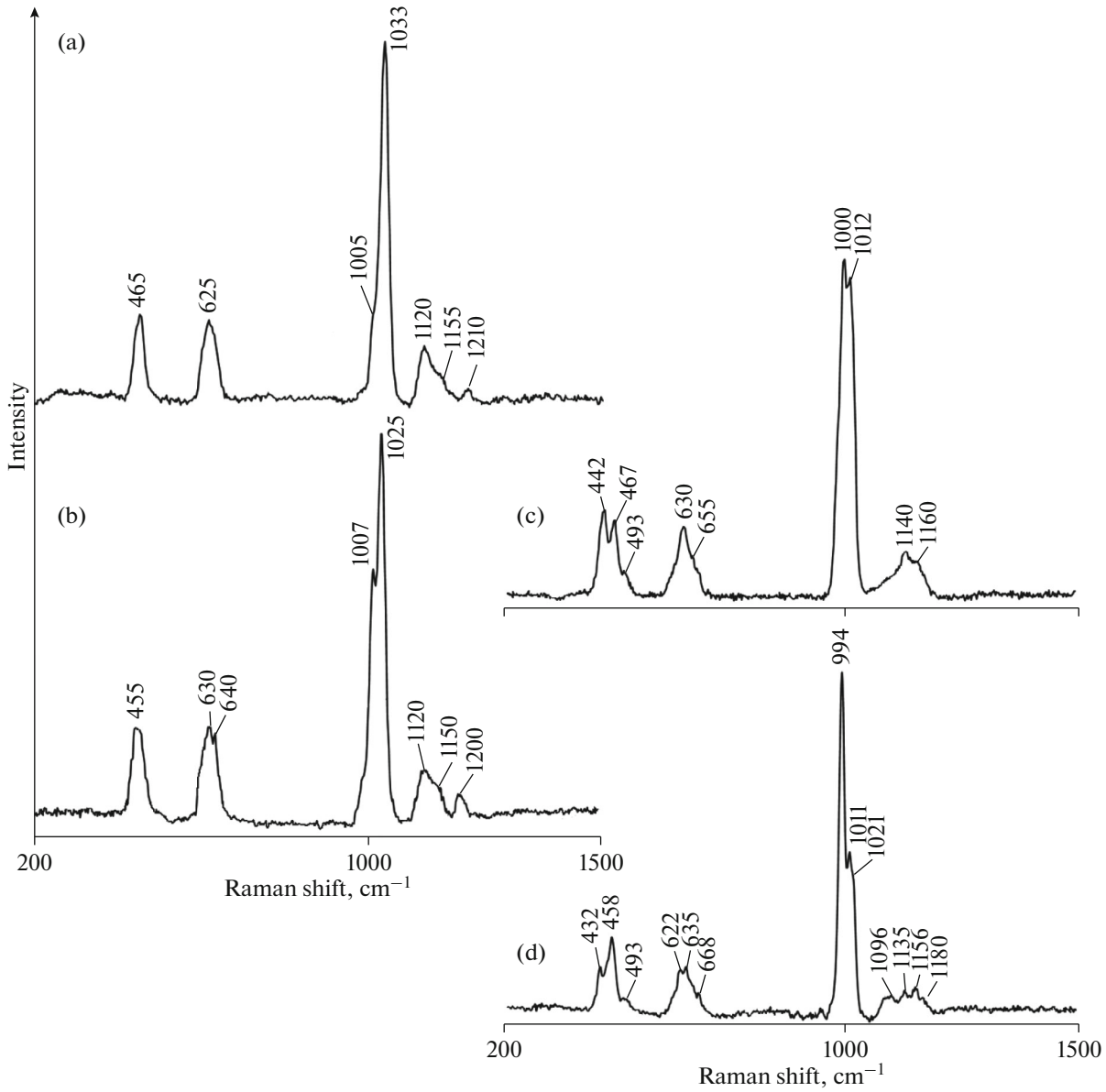

Fig. 10. Raman spectra of (a, b) calciolangbeinite-*C* and (c, d) calciolangbeinite-*O* with various compositions from fumarolic exhalations of the Tolbachik volcano (Kamchatka, Russia).

and Mg^{2+} in octahedral coordination in oxygen salts from fumarolic exhalations of Tolbachik is characteristic, for example, of grigorievite (Pekov et al., 2014), dravertite (Pekov et al., 2017), and arsenates of the alluodite group (Koshlyakova et al., 2018). However, it is still limited due to the fact that centered Cu^{2+} polyhedra tend to be significantly distorted due to the Jahn–Teller effect (Pekov et al., 2018b). For the same reason, copper is probably not included in large quantities in the langbeinite structure.

In a number of Tolbachik fumarole minerals, Cu^{2+} also exhibits isomorphism with large cations such as K, Na, and Pb, which was noted in aleutite, averievite, piypite, and romanorlovite (Pekov et al., 2018b); recently described and metatenardite containing up to 4.4 wt % of CuO (Shchipalkina et al., 2021). Based on these data, it can be assumed that Cu^{2+} in vanthoffite can enter not only the Mg^{2+} position, but also to a small extent replace Na^+ according to the heterovalent isomorphism scheme (probably with the formation of vacancies: $Cu^{2+} + \square^0 \rightarrow 2Na^+$).

For fumarolic langbeinite and calciolangbeinite, an admixture of sodium was very typical. The Na_2O concentration in some samples reaches 2.3 wt %. Isomorphic series $K_2Mg_2(SO_4)_3$–$Na_{1.8}K_{0.2}Mg_2(SO_4)_3$ with a cubic structure of langbeinite was obtained artificially (Trussov et al., 2019). As the degree of potassium substitution for sodium increases, in accordance with

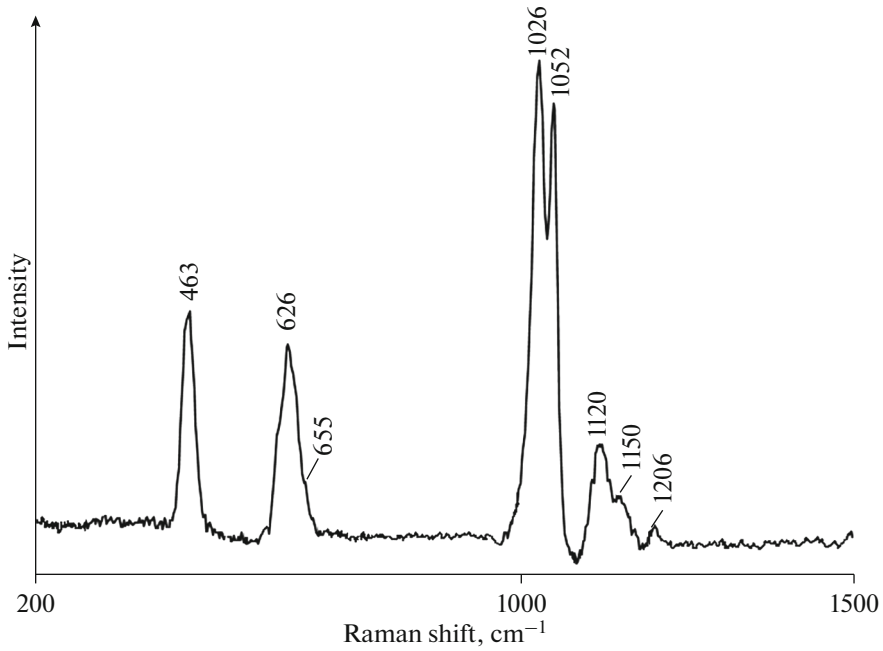

Fig. 11. Raman spectrum of sample which corresponds in gross composition to calciolangbeinite with 40 mol % $K_2Mg_2(SO_4)_3$ and contains breakdown structures (the Arsenatnaya fumarole, Tolbachik volcano).

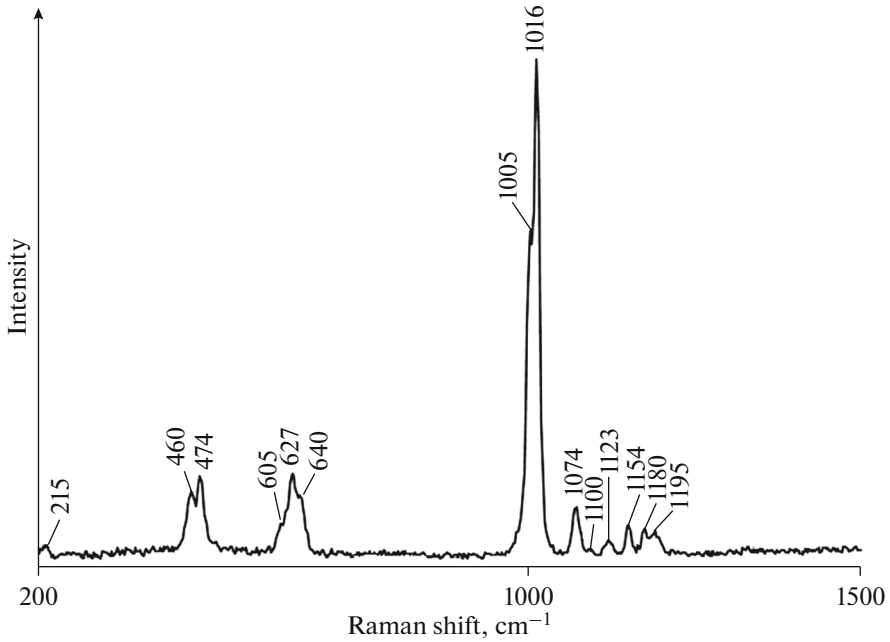

Fig. 12. Raman spectrum of vanthoffite from the Glavnaya Tenoritovaya fumarole (Tolbachik volcano) with composition $Na_{5.76}K_{0.01}Mg_{0.92}Zn_{0.07}S_{4.04}O_{16}$.

Vegard's rule, these phases exhibit a linear decrease in the unit cell size up to $a = 9.71$ Å and $V = 915.6$ Å^3 with the composition $Na_{1.78}K_{0.22}Mg_2(SO_4)_3$ (for langbeinite without impurities, $a = 9.92$ Å and $V = 977$ Å^3 (Mereiter, 1979)). Compounds with a Na content of > 1.8 a.f. acquire rhombic symmetry at room temperature with space group $P2_12_12_1$ (Trussov et al., 2019). In the Na-enriched variety of langbeinite with the empirical formula $(K_{1.79}Na_{0.22})_{\Sigma 2.01}(Mg_{1.83}Na_{0.09}Zn_{0.07}Ca_{0.01})_{\Sigma 2.00}S_{3.02}O_{12}$ from the Main Tenoritovaya Fumarole, parameter a (9.89 Å) and volume V (966.4 Å^3) of the unit cell also turned out to be smaller compared to those of "pure"

langbeinite. The Raman spectrum turned out to be close to the spectrum given in (Trussov et al., 2019) for the $K_{0.75}Na_{0.25}Mg_2(SO_4)_3$ phase: the band of symmetric stretching vibrations ν_1 near 1050 cm^{-1} is nonasymmetric and wider than that in the spectra of langbeinite without significant impurities. Neither powder X-ray diffraction nor Raman spectroscopy revealed any foreign phases in our samples: native sodium minerals (for example, vanthoffite or sulfates of the phthitalite group), which could hypothetically be present as ingrowths and accidentally captured by the electron beam during the microprobe analysis. All of these data support the fact that sodium is indeed included in the structure of Tolbachin langbeinite, partially replacing potassium. The occurrence of this element in position *M* with this small amount cannot be confirmed, but this possibility cannot be excluded.

In bulk chemical analyses of langbeinite from evaporites, Na is often present, but it is always accompanied by a comparable amount of Cl, and so the appearance of sodium in this mineral is associated with halite inclusions, which is also confirmed by stoichiometry and X-ray phase studies (Korobtsova, 1955). In the ammonium members of the langbeinite group, efremovite, and ferroefremovite, the Na_2O concentration is less than 0.2 wt % (Shcherbakova and Bazhenova, 1989; Kasatkin et al., 2021). Thus, sodium in natural sulfates of the langbeinite group was not reliably noted in such a large amount as in samples from Tolbachik's fumaroles.

In the fumaroles of Tolbachik, the minerals of the langbeinite group and vanthoffite crystallized probably during the interaction of hot volcanic gas with basalt. Based on the data on the relative volatility of various components in fumarole systems (Symonds and Reed, 1993; Zelenski et al., 2014), it can be concluded that Mg and Ca were most likely mobilized from the host rock, a source of K and S, and that impurity Cu, Zn, Cd, Rb, and Cs became a fumarole gas while Na, Fe, and Mn could both be introduced by the gas and come from basalt minerals, which in chambers with sulfate incrustations is intensively replaced by sanidine and cristobalite aggregates under the action of the gas. As shown in (Shchipalkina et al., 2021), vanthoffite can be also formed as a result of the decomposition of solid solutions in the Na_2SO_4–$MgSO_4$ system.

High temperatures of crystallization and enrichment of volcanic exhalations with a wide range of elements determined the peculiarity of the chemical composition of fumarolic langbeinite, calciolangbeinite, and vanthoffite.

ACKNOWLEDGMENTS

The authors are grateful to M.F. Vigasina for discussing the Raman spectra. The study of minerals by powder X-ray diffraction was carried out on the equipment of the Resource Center "X-ray Diffraction Methods of Research" of St. Petersburg State University.

FUNDING

This work was supported by the Russian Science Foundation, grant no. 19-17-00050.

CONFLICT OF INTEREST

The authors declare that they have no conflicts of interest.

REFERENCES

Abrahams, S.C. and Bernstein, J.L., Piezoelectric langbeinite-type $K_2Cd_2(SO_4)_3$. Room-temperature crystal structure and ferroelastic transformation, *J. Chem. Phys.*, 1977, vol. 67, pp. 2146–2150

Anthony, J.W., Bideaux, R.A., Bladh, K.W., and Nichols, M.C., *Handbook of Mineralogy. Volume 5. Borates, Carbonates, Sulfates*, Tucson: Mineral Data Publishing, 2003.

Babel, M. and Schreiber, B.C., Geochemistry of evaporates and evolution of seawater, In *Treatise on Geochemistry. Sediments, Diagenesis, and Sedimetary Rocks,* 2nd Ed., 2014, pp. 483–560.

Balić-Žunić, T., Garavelli, A., Jakobsson, S.P., Jonasson, K., Katerinopoulos, A., Kyriakopoulos, K., and Acquafredda, P., Fumarolic minerals: an overview of active European volcanoes*, Updates in Volcanology,—From Volcano Modelling to Volcano Geology,* Nemeth, K., Eds., IntechOpen, 2016, pp. 267–322.

Balić-Žunić, T., Pamato, M.G., and Nestola, F., Redetermination and new description of the crystal structure of vanthoffite, $Na_6Mg(SO_4)_4$, *Acta Crystal.*, 2020, vol. E76, pp. 785—789

Bellanca, A., Sulla simmetria della manganolangbeinite. Rendiconti dell`Accademia Nazionalic dei Lincei, *Classe di Scienze Fisiche, Matematiche e Naturali, Serie VIII*, 1947, vol. 2, pp. 451–455.

Britvin, S.N., Dolivo-Dobrovolsky, D.V., and Krzhizhanovskaya, M.G., Software for processing the X-ray powder diffraction data obtained from the curved image plate detector of Rigaku RAXIS Rapid II diffractometer, *Zap. Ross. Mineral. O-va*, 2017, vol. 3, pp. 104–117.

Chesnokov, B.V. and Shcherbakova, E.P., *Mineralogiya gorelykh otvalov Chelyabinskogo ugol'nogo basseina (opyt mineralogii tekhnogeneza)* (Mineralogy of Burnt Dumps of the Chelyabinsk Coal Basin (Experience of Technogenesis Mineralogy)), Moscow: Nauka, 1991.

Devarajan, V. and Salje, E., Phase transition in $K_2Cd_2(SO_4)_3$: investigation of non-linear dependence of spontaneous strain and morphic birefringence on order parameter as determined from excess entropy measurements, *J. Phys. Chem.*, 1984, vol. 17, pp. 5525–5537.

Fischer, W. and Hellner, E., Ueber die struktur des vanthoffits, *Acta Cryst.*, 1964, vol. 17, p. 1613.

Galuskin, E.V., Galuskina, I.O., Gfeller, F., Kruger, B., Kusz, J., Vapnik, Y., Dulski, M., and Dzierzanowski, P., *Silicocarnotite*, $Ca_5[(SiO_4)(PO_4)](PO_4)$, a new "old" mineral from the Negev Desert, Israel, and the ternesite–silicocarnotite solid solution: indicators of high-temperature alteration of pyrometamorphic rocks of the Hatrurim Com-

plex, Southern Levant, *Eur. J. Mineral.*, 2016, vol. 28, pp. 105–123.

Galuskina, I.O., Vapnik, Y., Lazic, B., Armbruster, T., Murashko, M., and Galuskin, E.V., Harmunite Ca-Fe_2O_4: A new mineral from the Jabel Harmun, West Bank, Palestinian Autonomy, Israel. *Am. Mineral.*, 2014, vol. 99, pp. 965–975.

Gattow, G. and Zemann, J., Uber doppelsulfate vom langbeinit-typ, $A_2^+B_2^{2+}(SO_4)_3$, *Zeitschrift fur Anorganische Allgemeine Chemie*, 1958, vol. 293, pp. 233–240.

Hikita, T., Sato, S., and Ikeda, T., Phase transitions in some langbeinite-type compounds, *J. Phys. Soc. Japan*, 1977, vol. 42, pp. 1656–1659.

Ivanov, A.A. and Voronova, M.L., *Galogennye formatsii (mineral'nyi sostav, tipy i usloviya obrazovaniya; metody poiskov i razvedka mestorozhdenii mineral'nykh solei)* (Halogen Formations (Mineral Composition, Types and Conditions of Formation; Methods of Prospecting and Exploration of Mineral Salt Deposits), Moscow: Nedra, 1972.

Kasatkin, A.V., Plášil, J., Škoda, R., Campostrini, I., Chukanov, N.V., Agakhanov, A.A., Karpenko, V.Y., and Belakovskiy, D.I., Ferroefremovite, $(NH_4)_2Fe_2(SO_4)_3$, a new mineral from Solfatara di Pozzuoli, Campania, Italy, *Can. Mineral.*, 2021. Vol. 59, no. 1, pp. 59–68.

Khod'kova, S.V., Langbeinite of the Carpathian region and its parageneses (on the example of the Stebnik deposit, *Litol. Polezn. Iskop.*, 1968, no. 6, pp. 73–85.

Korobtsova, M.S., *Mineralogy of potash deposits of the Eastern Carpathian region*, *Voprosy mineralogii osadochnykh obrazovanii* (Problems of Mineralogy of Sedimentary Rocks), 1955, vol. 2, pp. 3–137.

Košek, F., Culka, J., and Jehlička, A., Raman spectroscopic study of six synthetic anhydrous sulfates relevant to the mineralogy of fumaroles, *J. Raman Spectroscop.*, 2018. https://doi.org/10.1002/jrs.5363

Koshlyakova, N.N., Zubkova, N.V., Pekov, I.V., Giester, G., and Sidorov, E.G., Crystal chemistry of johillerite, *Can. Mineral.*, 2018, vol. 56, pp. 189–201.

Kubierschky, K., *Über ein Eigenthumliches Salzvorkommen im Sogenannten Magdeburg-Halberstädter Becken*, Berlin: Sitzungsberichte der Koniglich Preussischen Akademie der Wissenschaften, 1902, pp. 404–413.

Lander, L., Rousse, G., Batuk, D., Colin, C., Alves, C., Corte, D., and Tarascon, J.-M., Synthesis, structure and electrochemical properties of K-double sulfates $K_2M_2(SO_4)_3$, with M = Fe and Cu, *Inorg. Chem. (Amer. Chem. Soc.)*, 2017, vol. 56, no. 4, pp. 2013–2021.

Latush, L.T., Rabkin, L.M., Torgashev, V.I., Shuvalov, L.A., and Brezina, B., Raman spectra and phase transitions in some langbeinites, *Ferroelectrics*, 1983, vol. 48, pp. 247–258.

Martynov, K.V., Tananaev, I.G., Nekrasov, A.N., and Kotel'nikov, A.R., Synthesis and study of the chemical stability and strength of zirconium phosphates with the structure of langbeinite with imitators of highlevel radioactive waste (HLRW), *Glass Phys. Chem.*, 2017, vol. 43, no. 1, pp. 75–82.

Masalehdani, N.-N.M., Mees, F., Dubois, M., Coquinot, Y., Potdevin, J.-L., Fialin, M., and Blanc-Valleron, M.-M., Condensate minerals from a burning coal-waste heap in Avion, Northern France, *Can. Mineral.*, 2009, vol. 47, pp. 573–591.

Mereiter, K., Refinement of the crystal structure of langbeinite, $K_2Mg_2(SO_4)_3$, *Neues Jahrb. Mineral., Monatsh.*, 1979, no. 4, pp. 182–188.

Mitolo, D., Garavelli, A., Pedersen, L., Balic-Zunic, T., Jakobsson, S.P., and Vurro, F., Mineralogy of actually forming sublimates at Eldfell Volcano, Heimaey (Vestmannaeyjar archipelago), Iceland, *Plinius*, 2008, vol. 34, p. 322.

Morey, G.W., Rowe, J.J., and Fournier, R.O., The system $K_2Mg_2(SO_4)_3$ (langbeinite)–$K_2Ca_2(SO_4)$ (calcium–langbeinite), *J. Inorg. Nucl. Chem.*, 1964, vol. 26, pp. 53–58.

Nakamoto, K., *Infrared and Raman Spectra of Inorganic and Coordination Compounds. Part A*, 6th Edition, New Jersey: Wiley & Sons, 2009.

Nguyen, T.Ch., Lobanova, V.V., and Frank-Kamenetsky, V.A., The first discovery of vanthoffite in salt deposits of the Eastern Carpathian region, *Zap. Vsesoyuz. Mineral. O-va*, 1973, vol. 102, no. 2, pp. 192–193.

Parafiniuk, J. and Kruszewski, Ł., Ammonium minerals from burning coal-dumps of the Upper Silesian Coal Basin (Poland), *Geol. Quarter.*, 2009, vol. 53, pp. 341–356.

Pekov, I.V., Zubkova, N.V., Agakhanov, A.A., Yapaskurt, V.O., Chukanov, N.V., Belakovskiy, D.I., Sidorov, E.G., and Pushcharovsky, D.Yu., Dravertite, $CuMg(SO_4)_2$, a new mineral species from the Tolbachik volcano, Kamchatka, Russia,*Eur. J. Mineral.*, 2017, vol. 29, no. 2, p. 323.

Pekov, I.V., Zubkova, N.V., Galuskina, I.O., Kusz, J., Koshlyakova, N.N., Galuskin, E.V., Belakovskiy, D.I., Bulakh, M.O., Vigasina, M.F., Chukanov, N.V., Britvin, S.N., Sidorov, E.G., Vapnik, Y., and Pushcharovsky, D.Yu., Calciolangbeinite $K_2Ca_2(SO_4)_3$, a new mineral from the Tolbachik volcano, Kamchatka, Russia, *Mineral. Mag.*, 2012, vol. 76, no. 3, pp. 673–682. https://doi.org/10.1180/mgm.2021.95

Pekov, I.V., Zubkova, N.V., Yapaskurt, V.O., Britvin, S.N., Vigasina, M.F., Sidorov, E.G., and Pushcharovsky, D.Yu., New zinc and potassium chlorides from fumaroles of the Tolbachik volcano, Kamchatka, Russia: mineral data and crystal chemistry. II. Flinteite, K_2ZnCl_4, *Eur. J. Mineral.*, 2015, vol. 27, pp. 581–588.

Pekov, I.V., Zelenski, M.E., Zubkova, N.V., Yapaskurt, V.O., Chukanov, N.V., Belakovskiy, D.I., and Pushcharovsky, D.Yu., Calciolangbeinite $K_2Ca_2(SO_4)_3$, a new mineral from the Tolbachik volcano, Kamchatka, Russia. *Mineral. Mag.*, 2012, vol. 76, no. 3, pp. 673–682

Pekov, I.V., Zubkova, N.V., Yapaskurt, V.O., Kartashov, P.M., Polekhovsky, Yu.S., and Murashko, M.N., Pushcharovsky, D.Yu., Koksharovite, $CaMg_2Fe_4^{3+}$, and grigorievite, $Cu_3Fe_2^{3+}$, two new howardevansite-group minerals from volcanic exhalations, *Eur. J. Mineral.*, 2014, vol. 26, no. 5, pp. P. 667–677.

Pekov, I.V., Koshlyakova, N.N., Zubkova, N.V., Lykova, I.S., Britvin, S.N., Yapaskurt, V.O., Agakhanov, A.A., Shchipalkina, N.V., Turchkova, A.G., and Sidorov, E.G., Fumarolic arsenates—a special type of arsenic mineralization, *Eur. J. Mineral.*, 2018a, vol. 30, no. 2, pp. 305–322.

Pekov, I.V., Zubkova, N.V., and Pushcharovsky, D.Yu., Copper minerals from volcanic exhalations—a unique family of natural compounds: crystal chemical review, *Acta Crystallographic.*, 2018b, vol. B74, pp. 502–518.

Pekov, I.V., Agakhanov, A.A., Zubkova, N.V., Koshlyakova, N.V., Shchipalkina, N.V., Sandalov, F.D., Yapaskurt, V.O., Turchkova, A.G., and Sidorov, E.G., Oxidizing-type fumaroles of the Tolbachik Volcano, a mineralogical and geochemical unique, *Russ. Geol. Geophys.*, 2020, vol. 61, nos. 5–6, pp. 675–688.

Pekov I.V., Zubkova N.V., Galuskina I.O., Kusz J., Koshlyakova N.N., Galuskin E.V., Belakovskiy D.I., Bulakh M.O., Vigasina M.F., Chukanov N.V., Britvin S.N.,

Sidorov E.G., Vapnik Y., and Pushcharovsky D.Yu., Calciolangbeinite-O, a natural orthorhombic modification of $K_2Ca_2(SO_4)_3$, and the langbeinite-calciolangbeinite solid-solution system, Miner. Mag, 2022, vol. 86, no. 4, pp. 557–569.

Popova, V.I. and Popov, V.A., Crystal morphology of some exhalation minerals of the Great Fissure Tolbachik Eruption (Kamchatka), *Ural'sk. Mineral. Sb.*, 1995, no. 5, pp. 235–245.

Ramsdell, L.S., An X-ray study of the system K_2SO_4–$MgSO_4$–$CaSO_4$, *Am. Mineral.*, 1935, vol. 20, pp. 569–574.

Rowe, J.J., Morey, G.W., and Silber, C.C., The ternary system K_2SO_4–$MgSO_4$–$CaSO_4$, *J. Nucl. Chem.*, 1967, vol. 29, no. 4, pp. 925–942.

Russo, M., Campostrini, I., and Demartin, F., I minerali di origine fumarolica dei Campi Flegrei: Solfatara di Pozzuoli (Napoli) e dintorni, *Micro*, 2017, vol. 17, pp. 122–192.

Sejkora, J. and Kotrlý, M., Sulfáty vysokoteplotnı oxidačnı minerálnı asociace; hořıcı odval dolu Kateřina v Radvanicıch v Čechách, *Bull. Mineral.-Petrograf. Oddělen. Národnıho Muzea Praze*, 2001, vol. 9, pp. 261–267

Shannon, R.D., Revised effective ionic radii and systematic studies of interatomic distances in halides and chalcogenides, *Acta Cryst.*, 1976, vol. A32, pp. 751–767.

Shcherbakova, Y.P. and Bazhenova, L.F., Efremovite $(NH_4)_2Mg_2(SO_4)_3$—ammonium analogue of langbeinite—a new mineral, *Zap. Vsesoyuz. Mineral. O-va*, 1989, vol. 118, no. 3, pp. 84–87.

Shchipalkina, N.V., Pekov, I.V., Koshlyakova, N.N., Britvin, S.N., Zubkova, N.V., Varlamov, D.A., and Sidorov, E.G., Unusual silicate mineralization in fumarolic sublimates of the Tolbachik Volcano, Kamchatka, Russia,—Part 1: Neso-, cyclo-, ino- and phyllosilicates, *Eur. J. Mineral.*, 2020, vol. 32, no. 1, pp. 101–119.

Shchipalkina, N.V., Pekov, I.V., Britvin, S.N., Koshlyakova, N.N., and Sidorov, E.G., Alkali sulfates with aphthitalite-like structures from fumaroles of the Tolbachik volcano, Kamchatka, Russia. III. Solid solutions and exsolutions, *Can. Mineral.*, 2021, vol. 59, pp. 713–727.

Shimobayashi, N., Ohnishi, M., and Miura, H., Ammonium sulfate minerals from Mikasa, Hokkaido, Japan: boussingaultite, godovikovite, efremovite and tschermigite. *J. Mineral. Petrol. Sci.*, 2011, vol. 106, pp. 158–163.

Speer, D. and Salje, E., Phase transitions in langbeinites I. Crystal chemistry and structures of K-double sulfates of the langbeinite type $M_2^{++}K_2(SO_4)_3$, M^{++} = Mg, Ni, Co, Zn, Ca. *Phys. Chem. Mineral.*, 1986, vol. 13, pp. 17–24.

Stewart, F.H., *Marine evaporates: data of geochemistry, Geol. Surv. Prof. Pap.,* 1963, vol. 440-Y.

Stoiber, R.E. and Rose, W.I., Fumarole incrustations at active Central American volcanoes. *Geochim. Cosmochim. Acta*, 1974, vol. 38, pp. 495–516.

Symonds, R.B. and Reed, M.H., Calculation of multicomponent chemical equilibria in gas-solid-liquid systems: calculation methods, thermochemical data, and applications to studies of high-temperature volcanic gases with examples from Mount St. Helens, *Am. J. Sci.*, 1993, vol. 293, pp. 758–864.

Szakáll, S. and Kristály, F., Ammonium sulphates from burning coal dumps at Kolmó and Pécs-Vasa, Mecsek Mts., South Hungary, *Mineral., Spec. Pap.*, 2008, vol. 32, p. 154.

Tesfaye, F., Lindberg, D., Moroz, M., and Hupa, L., Investigation of the K–Mg–Ca sulfate system as part of monitoring problematic phase transformations in renewable-energy power plants, *Energies*, 2020, vol. 13, pap. 5366.

The Great Tolbachik Fissure Eruption, Fedotov, S.A. and Markhinin. Y.K., Eds., New York: Cambridge University Press, 1984.

Trussov, I.A., L.L. Male, Driscoll L.L., Sanjuan M.L. Synthesis and structures of sodium containing $K_{2-x}^{++}Na_xMg_2(SO_4)_3$ langbeinite phases, *J. Solid State Chem.*, 2019, vol. 276, pp. 37–46.

Vergasova, L.P. and Filatov, S.K., Minerals of volcanic exhalations—a new genetic group (using data on the Tolbachik volcano eruption in 1975—1976), *Zap. Vsesoyuz. Mineral. O-va*, 1993, vol. 122, no. 4, pp. 68–76.

Vergasova, L.P. and Filatov, S.K., A study of volcanogenic exhalation mineralization, *J. Volcanol. Seismol.*, 2016, vol. 10, no. 2, pp. 71–85.

Vishnyakov, A.K., Moskovskiy, G.A., Goncharenko, O.P., Vafina, M.S., Vershinin, D.S., and Sopivnik, I.V., Mineral composition of halogenic rocks of the Nivensky Basin of the Kaliningrad-Gdansk saliferous basin and conditions of its formation, *Litosfera*, 2016, no. 4, pp. 102–113.

Vlokh, R., Giryk, I., Vlokh, O.V., Skab, I., Say, A., and Uesu, Y., Once more about "forbidden" domain structure and the isolated point in in $K_2Cd_{2x}Mn_{2(1-x)}(SO_4)_3$ langbeinites, *Ukrain. J. Phys. Optics.*, 2004, vol. 5, no. 4, pp. 141–146.

Yamada, N., Maeda, M., and Adachi, H., *Structures of langbeinite-type K*, p. 2.

Yazhenskikh, E., Jantzen, T., Kobertz, D., Hack, K., and Muller, M., Critical thermodynamic evaluation of the binary sub-systems of core sulfate system Na_2SO_4–K_2SO_4–$MgSO_4$–$CaSO_4$, *Calphad*, 2021, vol. 72, pap. 102313.

Zambonini, F. and Carobbi, G., Sulla presenza, tra i prodotti dell'attuale attivita del Vesuvio, del composto $Mn_2K_2(SO_4)_3$, *Prendiconti della Regia Accademia delle Scienze Fisiche e Matematiche di Napoli*, 1924, vol. 30, pp. 123–126.

Zapeka, B., Klymiv, I.M., and Teslyuk, I., Phase transitions in As-grown $K_{0.2}Rb_{1.8}Cd_2(SO_4)_3$ langbeinite crystals: a birefringence study, *Ukrain. J. Phys. Optics*, 2013, vol. 14, no. 2, pp. 70–73.

Zelenski, M., Malik, N., and Taran, Yu., Emissions of trace elements during the 2012–2013 effusive eruption of Tolbachik volcano, Kamchatka: enrichment factors, partition coefficients and aerosol contribution, *J. Volcanol. Geotherm. Res.*, 2014, vol. 285, pp. 136–149.

Zemann, A. and Zemann, J., Die kristallstruktur von langbeinit, $K_2Mg_2(SO_4)_3$, *Acta Cryst.*, 1957, vol. 10, pp. 409–413.

Zuckschwert, S., Langbeinit, ein neues Kaliummagnesiumsulfat. In: *Deutsche Gesellschaft für Angewandte Chemie. Sitzungsberichte der Bezirksvereine. Bezirksverein fur Sachsen und Anhalt. Sitzung in Stassfurt, den 19, April 1891, Jahrgang*: Zeitschrift fur Angewandte Chem., 1891, pp. 354–356.

Translated by A. Ivanov